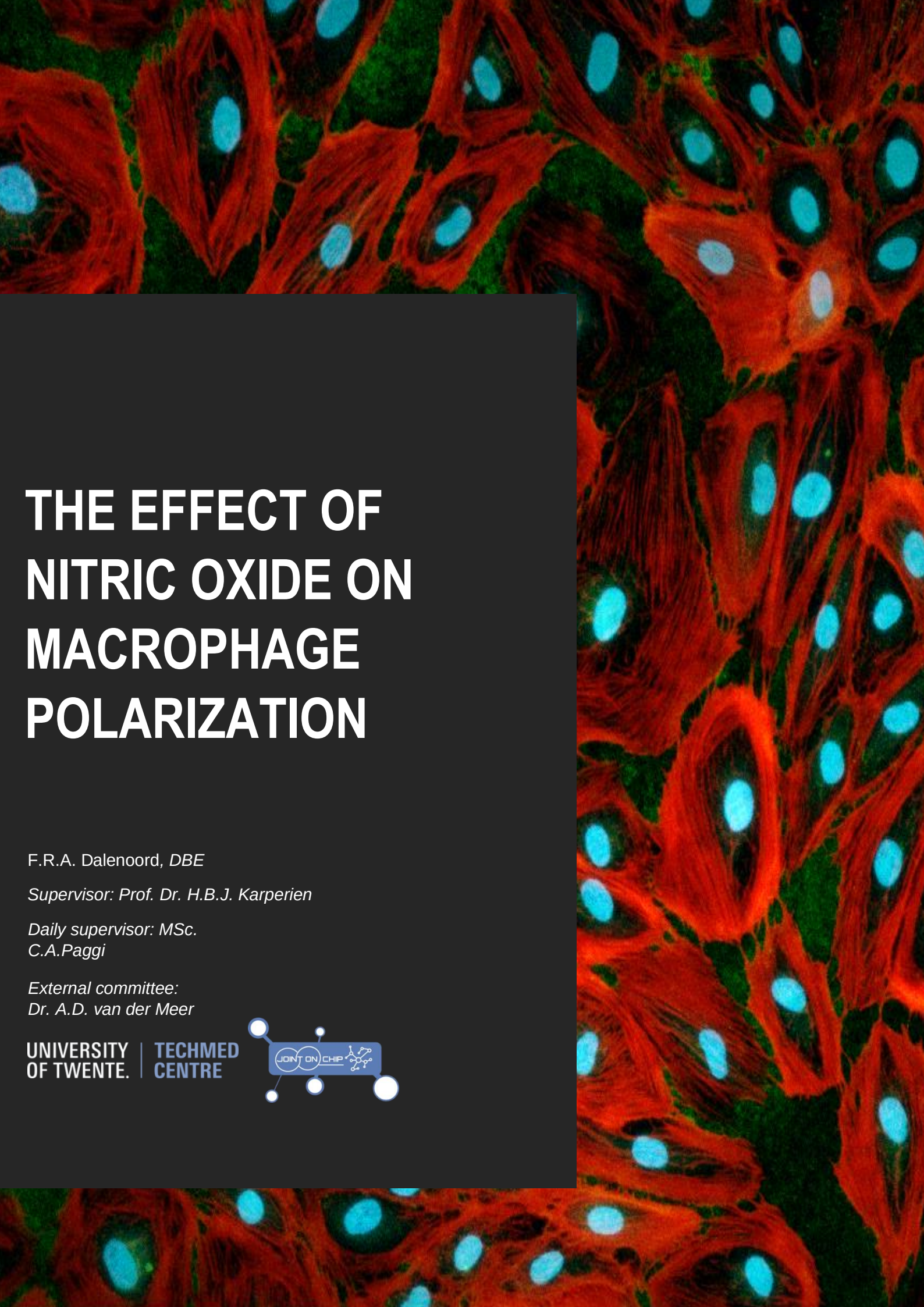

THE EFFECT OF NITRIC OXIDE ON MACROPHAGE POLARIZATION

F.R.A. Dalenoord, *DBE*

Supervisor: Prof. Dr. H.B.J. Karperien

Daily supervisor: MSc. C.A.Paggi

External committee: Dr. A.D. van der Meer

UNIVERSITY OF TWENTE. | TECHMED CENTRE

JOINT ON CHIP

UNIVERSITY OF TWENTE

THE EFFECT OF NITRIC OXIDE ON MACROPHAGE POLARIZATION

BACHELOR ASSIGNMENT

F.R.A. Dalenoord (s2114305)

Supervisor:
Prof. H.B.J. Karperien

Daily supervisor:
Msc. C A. Paggi

External commitee:
Dr. A.D. van der Meer

Research group:
Developmental BioEngineering

July 9, 2021

Contents

Abstact

Osteoarthritis (OA) and rheumatoid arthritis (RA) are two common chronic joint disorders that cause major disability and high healthcare costs worldwide. Due to aging and increase in obesity, the number of people affected by these diseases and its healthcare costs will increase in the coming years. The most affected joint for OA patients is the knee joint, while the metacarpophalangeal and proximal interphalangeal joints are most affected in RA. Within these synovial joints, the synovial membrane, which provides synovial fluid, is influenced both by OA and RA. A characteristic feature of these diseases is inflammation in the synovial membrane and a thicker synovial membrane, which is due to an influx of immune cells such as macrophages. In OA and RA these macrophages are polarized to an inflammatory state, which degrade the synovial joint in the whole. One of the recently discussed messenger molecules that seems to affect the polarization of macrophages, is nitric oxide. It is hypothesized to be a stimulator of polarization to pro-inflammatory macrophages. As this has not been investigated yet, the results could potentially provide crucial information on the development of OA and RA. In this report, the effect of nitric oxide on the polarization of macrophages in the synovial membrane is investigated.

A synovial membrane-on-chip system was used to mimic the synovial membrane. The device consists of two distinctive compartments, seperated by a PDMS membrane. The top chamber was filled with human synovial fibroblasts and macrophages and the bottom compartment with human umbilical vein endothelial cells (HUVECs). As controls, this culture is compared to a double culture (only synovial fibroblasts and macrophages) and a single culture (only synovial fibroblasts). To measure the concentration of nitric oxide (NO) a Griess assay was performed. Furthermore, both immunofluorescence and qPCR were performed to determine the polarization of the seeded macrophages and other extracellular matrix markers, such as collagen 1 (*COL1*) and hyaluronic acid synthase 1 (*HAS1*).

Partial to no integration of macrophages was visible 3 hours after seeding of macrophages in double culture samples and worsens over the days, while full integration was visible for triple culture samples (fibroblasts, macrophages and HUVECs). The Griess assay showed an increasing difference between double and triple culture samples. Double culture samples were high in NO, while triple culture samples were significantly low. Immunofluorescence showed clusters of collagen 1 in low concentrations of NO, which suggests higher amounts of tissue-regenerative macrophages. Moreover, more CD163 accentuated macrophages were visible in triple culture samples. qPCR results showed a higher gene expression of M2 markers for low NO levels, than high NO levels. IL1R, a M1 marker, showed a decrease in gene expression at low NO levels, while an increase was seen at high NO levels. While more research is needed to prove causality, it seems that low levels are coupled with a polarization to M2 macrophages and high levels of nitric oxide are coupled with polarization to M1 macrophages.

Samenvatting

Osteoartritis (OA) en reumatoïde artritis (RA) zijn twee veelvoorkomende chronische gewrichtsaandoeningen die wereldwijd leiden tot grote invaliditeit en hoge zorgkosten. Door de vergrijzing en de toename van obesitas zal het aantal mensen dat door deze ziekten wordt getroffen en de zorgkosten de komende jaren toenemen. Het meest aangetaste gewricht voor OA-patiënten is het kniegewricht, terwijl de metacarpofalangeale en proximale interfalangeale gewrichten het meest worden aangetast bij RA. Binnen deze synoviale gewrichten wordt het synoviale membraan, dat synoviale vloeistof levert, beïnvloed door zowel OA als RA. Kenmerkend voor deze ziekten is een ontsteking in het synoviale membraan en een dikker synoviaal membraan, die het gevolg is van een instroom van immuuncellen zoals macrofagen. Bij artrose en RA zijn deze macrofagen gepolariseerd tot een inflammatoire toestand, die het synoviale gewricht in het geheel afbreken. Een van de recent besproken boodschappermoleculen die de polarisatie van macrofagen lijkt te beïnvloeden, is stikstofmonoxide. Er wordt verondersteld dat het een stimulator is van polarisatie naar pro-inflammatoire macrofagen. Omdat dit nog niet is onderzocht, kunnen de resultaten mogelijk cruciale informatie opleveren over de ontwikkeling van artrose en RA. In dit rapport wordt het effect van stikstofmonoxide op de polarisatie van macrofagen in het synoviale membraan onderzocht.

Een synoviaal membraan-op-chip-systeem werd gebruikt om het synoviale membraan na te bootsen. Het apparaat bestaat uit twee onderscheidende compartimenten, gescheiden door een PDMS-membraan. De bovenste kamer was gevuld met menselijke synoviale fibroblasten en macrofagen en het onderste compartiment met endotheelcellen van de menselijke navelstrengader (HUVEC's). Als controle wordt deze kweek vergeleken met een dubbele kweek (alleen synoviale fibroblasten en macrofagen) en een enkele kweek (alleen synoviale fibroblasten). Om de concentratie stikstofmonoxide (NO) te meten, werd een Griess-assay uitgevoerd. Verder werden zowel immunofluorescentie als qPCR uitgevoerd om de polarisatie van de gezaaide macrofagen en andere extracellulaire matrixmarkers, zoals collageen 1 te bepalen. Verder werd zowel immunofluorescentie als qPCR uitgevoerd om de polarisatie van de gezaaide macrofagen en andere extracellulaire matrixmarkers, zoals collageen 1 (*COL1*) en hyaluronzuursynthase 1 (*HAS1*) te bepalen.

Gedeeltelijke tot geen integratie van macrofagen was 3 uur na het zaaien van macrofagen in dubbele kweekmonsters zichtbaar en verslechterde in de loop van de dagen, terwijl volledige integratie zichtbaar was voor drievoudige kweekmonsters (fibroblasten, macrofagen en HUVEC's). De Griess-assay toonde een toenemend verschil tussen dubbele en driedubbele kweekmonsters. Dubbele kweekmonsters waren hoog in NO, terwijl drievoudige kweekmonsters significant laag waren. Immunofluorescentie toonde clusters van collageen 1 in lage concentraties NO, wat duidt op grotere hoeveelheden weefselregeneratieve macrofagen. Bovendien waren meer CD163-geaccentueerde macrofagen zichtbaar in drievoudige kweekmonsters. qPCR-resultaten toonden een hogere genexpressie van M2-markers voor lage NO-niveaus dan hoge NO-niveaus. IL1R, een M1-marker, vertoonde een afname in genexpressie bij lage NO-niveaus, terwijl een toename werd gezien bij hoge NO-niveaus. Hoewel er meer onderzoek nodig is om causaliteit te bewijzen, lijkt het erop dat lage niveaus gepaard gaan met een polarisatie naar M2-macrofagen en dat hoge niveaus van stikstofmonoxide gepaard gaan met polarisatie naar M1-macrofagen.

1 Introduction

Osteoarthritis (OA) and rheumatoid arthritis (RA) are the most common joint diseases of the musculoskeletal system affecting the lives of millions globally. Approximately 7% by OA and between 0.1 to 2% of the global population is affected by RA worldwide [1] [2]. This includes nearly 1.5 million patients, for OA, and approximately another 259 thousand people for RA diagnosed just in the Netherlands in 2019. Due to aging and high increase in obesity among the population of the Netherlands, the number of people affected by RA and especially OA will likely increase in the coming years. Alongside a relatively high prevalence, 654 million for RA and a staggering 1.2 billion euros for OA was spent by healthcare in 2017 in the Netherlands [3] [4] [5]. It is clear that the increase of these diseases will have an even larger impact on health systems and healthcare in the following years. It is expected that OA will be the single greatest cause of disability in the population in 2030 [6].

Although not lethal, OA and RA cause severe pain, disability and inability to work, which is then translated in reduction of the quality of life. Although not completely understood, OA leads to an inflammatory reaction inside of the synovial membrane of the joint bringing to cartilage degradation. RA is caused by an auto-immune reaction of the body in the synovial joint, which directly forms an inflammatory reaction. Due to this reaction, immune cells such as macrophages and T-cells infiltrate the synovial membrane. The infiltrated immune cells generate neovascularization in the synovial membrane, which leads to an expansion of the synovial lining. This leads to bony erosions and cartilage degradation [4] [7] [8]. Although new treatments are discovered every year for RA, OA still remains a disease where palliative treatments, to reduce the pain, are the best option [9] [10]. Fortunately, there has been a wide range of research on OA, which could potentially give a cure to this discouraging disease. However, first the mechanisms behind this disease have to be studied prior to finding a cure as understanding the mechanisms of the disease can provide the knowledge for a potential cure. This report therefore will give an insight into one of these mechanisms, considering the effect of nitric oxide on the polarization of macrophages in the synovial membrane.

1.1 Synovial membrane

The synovial joint is an organ within the musculoskeletal system. It provides free motion for two bones that are connected with the joint's structure [11]. Synovial joints can be distinguished from others joints by the presence of synovial fluid, an articular capsule and a joint cavity [12]. The inner surface of a synovial joint is covered with connective tissue named synovial membrane. Aside from its filtering function, the role of the synovial membrane is to supply the joint with synovial fluid [12]. This viscous fluid, containing hyaluronic acid, lubricin, phagocytic cells and filtrate of blood plasma, is used to provide nutrients to some of the tissues within the joint (e.g cartilage) and to reduce friction during movement. Balance of the composition in the synovial fluid is crucial, because a change in concentration of one (or more) of these elements will change its consistency. Changing the consistency of the synovial fluid will decrease its function; to absorb shocks of movement and to supply nutrients to the joint. Hence, providing a continuous and correct synovial fluid to the joint prevents damage of the joint [11].

The synovial membrane consists of an intimal lining layer consisting of a double or triple layer of cells and a thicker synovial sublining layer. The intimal lining layer mainly consists of fibroblast-like synovial cells, which are responsible for the production of synovial fluid. Furthermore, macrophage-like synovial cells are present in the synovial membrane and account for all the other cells in the intimal lining layer. The intimal lining layer of the synovial membrane is exposed to the synovial fluid, which enables the macrophages to interact with the synovial fluid. Their function is to phagocyte the debris in the synovial fluid generated during movement, maintaining the joint's homeostasis. The synovial sublining layer consists of endothelial cells, adipose tissue and nondifferentiated fibroblasts [12]. Besides the synovial specialized cells in the intimal lining layer, the tissue is also well vascularized by the underlying sublining layer to supply the synovial membrane with its nutrients. Overall, the synovial membrane is a complex tissue containing distinctive cells that perform several tasks, i.e. fibroblasts provide the synovial fluid with its components, while macrophages phagocyte the debris in synovial fluid. The vascularization provides the fibroblasts and macrophages with its nutrients [13].

1.2 Synovial membrane in OA and RA

The formation of osteophytes is one of the most distinctive pathological changes in an OA affected synovial joint. Osteophytes are newly formed fragments of bone at the edges of the joint. An increase in macrophage-like synoviocytes has been proven to be the cause of formation of those osteophytes [14]. How macrophages are influenced or what they secrete as cytokines determines the environment of the synovial membrane and thus the synovial joint. Characteristic cytokines for OA can be divided in 3 categories. Catabolic cytokines, which contribute to the degradation of the synovial tissue for OA include TNF-α, IL-1β and IL-6, -8, -17 and -18. New research has shown that IL-15 contributes to the catabolic side of OA pathogenesis. Also PGE2, nitric oxide and MMP's such as MMP-1 and MMP-3 play a role in the degradation of cartilage for OA, caused by the secretion of these molecules in the synovial membrane. Next to catabolic cytokines, anabolic cytokines, promote proliferation of cartilage [15]. Osteophytes are therefore formed, when these anabolic cytokines are expressed in a big quantity [14]. TGF-β is the most important anabolic cytokine for OA, which is produced by fibroblast-like synoviocytes and also promotes the formation of osteophytes. Last, regulatory cytokines of OA are IL-4, -6, -10 and -13. These inhibit the catabolic cytokines from degrading synovial cartilage [15] [16] [17]. Adaptive immunity-related inflammatory cells are increased in the synovial membrane of RA patients. In RA synovium, the number of macrophages is greatly increased. Here, it influences cartilage degradation. Besides an increase in macrophages, a significant increase in other immune cells such as neutrophils, basophils and eosinophils is seen. Also, larger amounts of T- and B-cells are present in RA synovium. [33] For RA synovium, higher expression of IL-1β, -6, -8, -10 and TNF-α, TGF-β1 was found [18] [19] [20] [21]. Adhesion molecules such as ICAM-1 and VCAM-1 were expressed more in RA compared with similar OA synovium. Especially IL-8 and IL-10 were expressed significantly more in RA synovium than OA synovium. This is likely due to the fact that the onset of RA is a form of chronic inflammation [19]. Other molecules, such as GM-CSF and MMP's are found in both OA and RA synovium [20] [21].

1.3 Macrophage polarization

Macrophages are the most highly present immune cells in our body. The monocyte, shown in figure 1, is the precursor of a macrophage. It is mostly found in the blood where it diffuses into tissues and differentiates into the commonly known M0 macrophage [11] [22] [23]. This leukocyte can have multiple functions when polarized, such as tissue repair and homeostastic maintenance in the body. Also, during inflammation, polarized macrophages play a key role in enhancing or reducing the inflammation. Their role is determined by their polarization. Macrophages can polarize in different ways. One way is by classical activation (M1), which gives rise to a pro-inflammatory macrophage. Another route is by alternative activation (M2), which generates an anti-inflammatory macrophage that can stimulate tissue repair. The polarization involves a variety of cytokines and other molecules that regulate the balance of M1/M2 polarization. In general, M1 polarization can be triggered by interferon gamma (IFN-γ) and lipopolysaccharides (LPS), two examples of the cytokines that trigger an inflammation reaction. M1 macrophages are distinguishable by their surface proteins, such as IL1R and CD80. Furthermore, M1 secretes certain proteins and cytokines, such as interleukins and chemokines [23] [24] [25]. [26] Another example of a gene expressed by M1 macrophages is inducible nitric oxide synthase (iNOS).

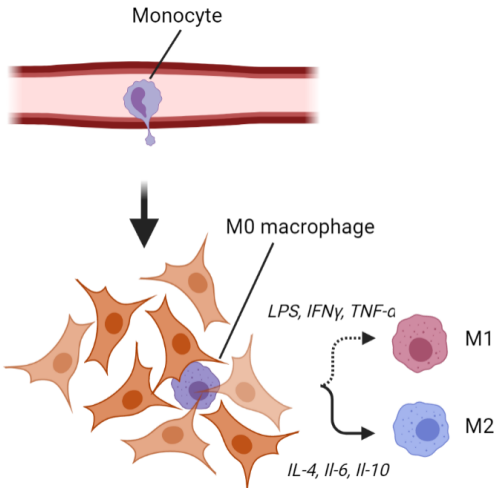

Figure 1: A monocyte is the precursor of a macrophage. When diffused through a blood capillary into tissue, it becomes a M0 macrophage. In the tissue, it can polarize into two states, M1 and M2. Polarization is stimulated by shown molecules for M1 and M2 macrophages.

M2 polarization is mainly triggered by interleukin 4 (IL-4) and interleukin 13 (IL-13) [23]. M2 macrophages can be classified into 4 subgroups, as shown in figure 2. These subgroups consist of M2a, M2b, M2c and M2d macrophages [23]. The 4 types of macrophages have different functions in our body, such as tissue repair for M2a and phagocytosis of apoptotic cells for M2c macrophages. They can be distinguished by their surface markers and their secreted cytokines. M2a has a distinguishable CD200R1 surface marker, whereas M2b has SPHK1 as a marker and M2c has an overexpression of TLR1 and TLR8 surface markers. M2d overexpresses VEGFα. [23] A cytokine that is secreted for all M2 subgroups is IL10. All macrophages express CD68 as a surface marker [25] [27] .

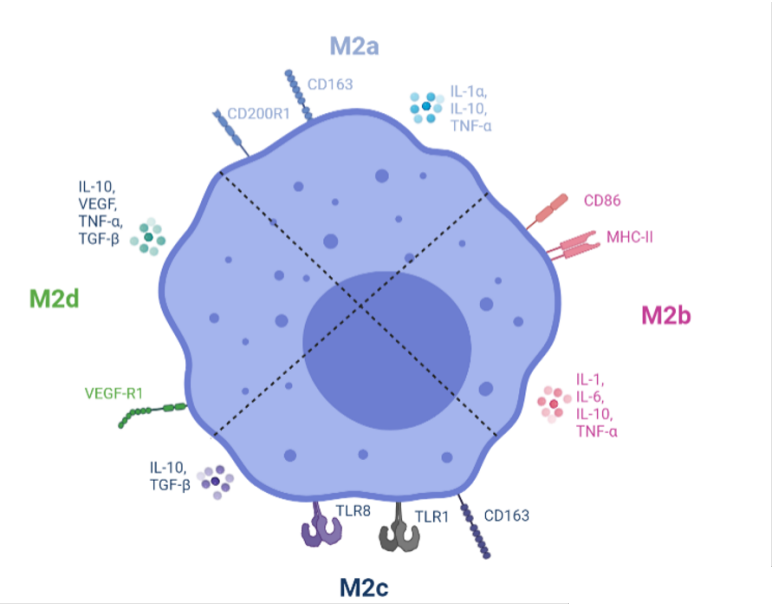

Figure 2: A M2 macrophage has 4 different subgroups. These different subgroups have different surface proteins and secrete distinguishable cytokines.

1.4 Nitric oxide production and detection

Nitric Oxide (NO) is a gaseous radical involved in multiple signaling pathways of organisms [28]. As NO has a very short physiological half-life [29], it needs to be produced continuously to maintain homeostasis. Nitric oxide synthase (NOS) is the key element in production of NO. NOS has three isoforms: endothelial NOS (eNOS), neuronal NOS (nNOS) and inducible NOS (iNOS) [30]. All forms of NOS use l-arginine and oxygen to produce NO and l-citrulline [31]. eNOS is mostly found in endothelial tissue, were it provides NO for en-

dothelial cells. NO functions here as a vasodilator, by binding to soluble guanylyl cyclase (sGC) that triggers muscle relaxation [28]. iNOS is an enzyme that is expressed in, for example, macrophages and is upregulated by IFN-γ and LPS. When produced in macrophages, NO reacts with the radical O_2^-. As a product, $ONOO^-$ is formed that damage pathogens as a powerful oxidant [32]. nNOS is a form of NOS that can be found in the neurovascular and skeletal muscle cells. All forms of NOS can be inhibited by L-NMMA [33] [31] [34] [35]. Furthermore, NO-donors can hand off NO, which will cause a rise in the concentration of NO [36] [35].
Unfortunately, the short psychological half-life of NO makes it hard to analyze for quantitive research. Therefore, an alternative method needs to be used to analyze the production or quantity of NO in samples. One possible alternative is to measure one or both derivatives of NO. Nitrite (NO_2) and nitrate (NO_3) are NO metabolites that have a significantly longer physiological half-life and therefore are measurable [37]. Three different methods are currently used for the detection of this molecule [38]. Colorimetric determination is one of these analysis methods. The Griess Assay is one of the most common method for colorimetric determination. Only NO2 is measured, by using nitrate reductase. Nitrite is then coupled to form a chromophoric azoproduct. This product can then be measured with an absorbance platereader.. Next, fluorometric determination, where DAF-2A is the most commonly used fluorescent. This technique uses a triazole fluorescent derivative. This compound can then be measured with a fluorescence plate reader. Besides this method having a high sensitivity, it is reasonably low in its cost-efficiency. However, the DAF family of fluorometric staining has not been used excessively in research with NO or its derivates, when compared to the colorimetric Griess reagent. Lastly, a spectrophotometric method can be used for quantitative research, which provides the most reliable determination of quantitative research concerning NO. Spectrophotometric methods use a radiant energy that is added to the solution. This energy is absorbed by NO and quickly emitted back again in a form of light. The amount of photon energy can be measured and therefore the NO can be measured. Unfortunately, this method is still hard to use for an inexperienced user. Thus it takes a substantial amount of time to get used to the method and present reliable results [38].

1.5 Current in vitro models and organ-on-chip

Ranging from 2D to 3D, rat cells to human cells and single cell line cultures to a coculture model; a wide variety of experiments has already been done on OA and RA through the years. These models present advantages and disadvantages [27] [39]. Monolayer osteoarthritis models are inexpensive, have a high throughput and expose the cells to an equal layer of nutrients. However, 2D monolayer models also have considerable disadvantages, such as a poor perspective of the reality and thus a very low possibility of a potential cure [39]. Monolayer coculture models have already a higher physiological proximity, but still lack the environmental fidelity as tissues are based on a three-dimensional model [27] [39]. 2D cocultures, such as a transwell plate with synoviocytes, adipose-derived stem cells and chondrocytes on different levels, showed that pro-inflammatory cytokines decrease in their expression when these cells interact with eachother [39], by cell-to-cell contact. Nonetheless, 3D models provide a number of solutions to some of the limitations of 2D models. 3D cell models include explants, which are surgically derived from human tissues. Synovial tissue can be surgically derived from osteoarthritic patients. These ex-vivo tissues or explants present major advantages with respect to the other models as the environmental fidelity is high. Also, tissue from explants is easy to gather, as only a surgical asportation and fixation of the sample has to be done. Moreover, explants can already have a 3D structure and can be used to better mimic disease onset (RA & OA). They do, however, present disadvantages as the tissues source is scarce with possible tissue damage during surgical asportation [27].

A human-joint-on-chip is seen as the next-generation preclinical in vitro screening system, that can mimic the nature of the disease. Rothbauer et al. [40] showed promising techniques for synovial membrane on chip. The use of patient derived primary synoviocytes showed a reliable synovium-on-chip system containing generated 3D synovial organoids. These systems can potentially serve as a reliable rapid screening tool for diseases such as inflammatory arthritis. An organ-on-chip system as several advantages. One of them is the ability to adjust important parameters, such as the biochemical or mechanical environment. Hence, the designer of the system can change the system to his experiment. For example, implementing mechanical stimulation to the system will change the behaviour of the cells in the system and this can be analyzed. Next, the through-put of the system is substantially higher, as experiments only need minimal amounts of cells and materials. Also, the possibility to combine different tissues makes these systems an excellent candidate to mimic an in vivo

situation. [27] [41]

In this report, a 3D scaffold model will be used, which provides a coculture for optimal cell-to-cell contact between macrophages and fibroblasts, while no cell-to-cell contact will be present between this coculture and HUVEC cells. The synovial membrane, for example, can be studied in this microenvironment by creating a multiple compartment systems that provides an in vitro 3D structure of the different tissues in the synovial membrane. However, an organ-on-chip also comes with disadvantages. As one can imagine, a cell culture done by such a system is challenging to design and implement compared to 2D in vitro experiments. Also, scaling up is hard to do as multiple mechanisms and interactions in a microenvironment are altered in a macroenvironment such as the body itself. [27] [41]

1.6 The aim of the project

The importance of NO and its signaling mechanisms is clearly described in a wide range of literature. In short, NO is a messenger molecule that leads to major mechanisms in tissues, including immunity and inflammation. However, little is known about the effect of NO in healthy and diseased (OA and RA) synovium. Hence, we aim at determining the effect of NO production in double or triple culture systems using a synovial membrane-on-chip. Furthermore, we wanted to control how this culture influence macrophages polarization and protein production.

2 Materials & Methods

Device fabrication
PDMS (poly(dimethylsiloxane)) was made by combining monomer and cross-linker in a 20:1 ratio. After mixing the monomer and cross-linker, the mix was degassed by a vacuum bell jar. PDMS was poured in a mold and degassed. The PDMS poured molds were placed in an oven at 67°C for 24 hours. The PDMS was cut out of the mold and holes of 2 mm thickness were punched to create the inlets in the system. Glass slides were covered with PDMS and cured at 67°C for 24 hours. A system presenting the punched inlets was then bonded to cured PDMS on a glass slide in a plasma oven at 500 mTorr, 50 W for 40 s. The system was peeled from the glass slide by cutting around the system on the glass slide. The bonded PDMS over the bottom compartment inlets was removed and the system is bonded to another second chip as shown in figure 3 in a plasma oven at 500 mTorr, 50 W for 40 s.

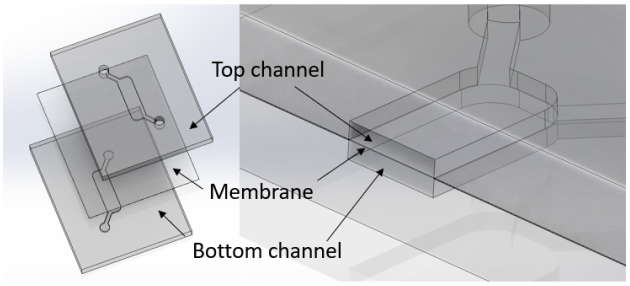

Figure 3: Solidwork design of the used microfluidic system in a 3D view. The system consist of a sandwich structure presenting a top and bottom channel separated by a thin PDMS non-porous membrane. This image is designed by C.A. Paggi

Device preparation
Polydopamine was made by adding 4 mg dopamine and 2 mL Tris-HCl buffer. 20 µL of polydopamine was added to both top and bottom compartments of the system. After 30 minutes, the polydopamine was removed and the channels were washed twice with PBS. After washing, 20 µL Collagen I was added to both channels in the system and incubated for 30 minutes at 37 °C and 5% CO2. Next, the unattached collagen I was removed and the channels were washed twice with PBS. 50 µL of PBS was left on top of the channels to prevent drying.

Cell culture fibroblasts
Thawed cells etc Synovial fibroblasts were cultured in a T175 flask, with 20 mL medium. Medium consisted of Dulbecco's modified eagle medium (DMEM, Thermofisher), 10% fetal bovine serum (FBS, Thermofisher) and 1% penicillin-streptomycin (pen/strep, Thermofisher). Medium was refreshed every 2 to 3 days. After culture, medium was removed and cells were washed with phosphate buffered saline (PBS, Thermofisher). Trypsin-EDTA (Invitrogen) was added to the cells for 5 minutes. After trypsinization, 6 mL of the described medium was added to the cells to neutralize the trypsinization. Cells were then brought in a 15 mL tube. Another 5 mL was added to the T175 flask to remove the remaining cells in the flask and added to the 15 mL tube. Cells were counted by adding 10 µL to a counting chamber. Cells were counted and the total amount of cells were calculated by the following formula:

$$Total amount of cells = counted cells in a single 1mm^2/4 * 1000 * milliliter of suspension + 300000$$

As the desired concentration is 2.5 million cells per mL, the total amount of cells is divided into 2.5 million to get the desired mL's of medium that needs to be added to the cell pellet. The cell suspension was then centrifugated at 500g for 3 minutes and medium was removed from the cell pellet. The calculated amount of medium was added to the cell pellet and resuspended to form a homologous cell suspension. 10 µL of cell suspension was then added to the top chamber of the system.

Cell culture macrophages
THP-1 monocytes were cultured in T25 flasks with 5 mL Roswell Park Memorial Institute (RPMI, Gibco)

medium. Medium consisted of glucose, phenol red, amino acids and vitamins. Phorbol myristate acetate (PMA) was added in a ratio of 1:1600 PMA:cell suspension solution. The cells with PMA added were cultured for 24 hours. Medium was removed after the 24 hour incubation. 20 mL of new media was added in the T175 flask. Cells were scraped off the bottom of the flask and suspended in a new 50 mL tube. Another 10 mL of RPMI medium was added to the culture flask and suspended in the 50 mL tube. Cells were pipetted through a 40 µm cell strainer 3 times. Cells were then counted in a Neubauer cell counter. Cells were centrifuged for 5 minutes at 300g.. New medium was added to get the right amount of cells per milliliter, which is 5000 per sample. Cells were then seeded into the top chamber of the system.

Cell culture HUVECs

Human Umbilical Vascular Endothelial Cells (HUVECs) were cultured in T75 flasks with 15 mL HUVEC medium. The HUVEC medium used was Endothelial Cell Growth Medium 2 (PromoCell, Germany). Cells were cultured at 37°C and 5% CO2. Medium was refreshed every 2 days. Medium was removed and cells were washed with PBS. 3 mL of Trypsin-EDTA was added to the cells and incubated at 37°C and 5% CO2 for 5 minutes. The collected substance was added to a 15 mL tube. Cells were counted as described earlier. Cell suspension was then centrifuged for 5 minutes at 300g. New medium was added to get the right amount of cells per milliliter, which is 50000 cells per sample. Cells were then seeded into the bottom chamber of the system with 20 µL cell suspension per sample. Droplets of the described medium was then poured on the bottom of the petri dish to prevent drying of the system. Samples were flipped and put on top of the droplets media. Petri dish was wrapped with parafilm and samples were incubated for 1 hour at 37 °C and 5% CO2. Samples were flipped again and remaining media on petri dish was removed. Cells were again seeded in the bottom chamber of the system with 20 µL cell suspension per sample. This procedure is done to cover the bottom chamber with HUVEC cells. In this way, a lumen of HUVEC cells is formed.

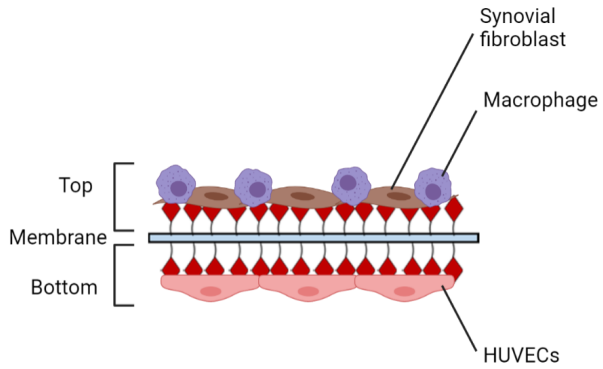

Figure 4: Schematic view of the different cell types seeded in the system. The top compartment is seeded with both synovial fibroblasts and macrophages, whereas the HUVEC cells are seeded in the bottom compartment.

Medium Refreshment

Media of samples was refreshed the day after seeding. After this, medium was refreshed every 2 days. Media was removed from the cells and new media consisting of 50% RPMI medium and 50% HUVEC medium. Droplets of media were put on top of the samples to prevent drying.

Griess assay

Griess Reagent System (Promega Corporation, USA) was used for the colorimetric assay and determination of the nitrite concentration [44]. The nitrite standard curve was made prior to the nitrite determination in the samples, as described in the protocol [42]. 5 µL of Sulfanilamide (Griess Reagent System, Promega Corporation USA) was pippetted into the top channel of the system. Samples were incubated at room temperature for 10 minutes in the dark. 5 µL of NED Solution (Griess Reagent System, Promega Corporation USA) was pippetted into the top channel of the system and again incubated for 10 minutes at room temperature in the dark. 15 µL of suspension was then sucked up out of the system and transformed into the 94 wells plate, next to the wells referred to the reference curve. The total suspension of 5 samples, which is 75 µL, corresponds for one well in the 96 wells plate. For day 6 and 8, this came to a total of 10 samples (two wells) per condition and on day 10 5 samples (one well) per condition. Absorbance of the samples was measured in 30 minutes with a plate

reader. Absorbance of the reference samples are plotted on a graph to form a curve according to [42]. This reference curve exists of a series of measurements with fixed concentrations of nitrite. The curve of reference can be drawn through these lines. Finally, the measured absorbance of a sample can be read off with respect to the reference curve to find the concentration of nitrite found in a sample.

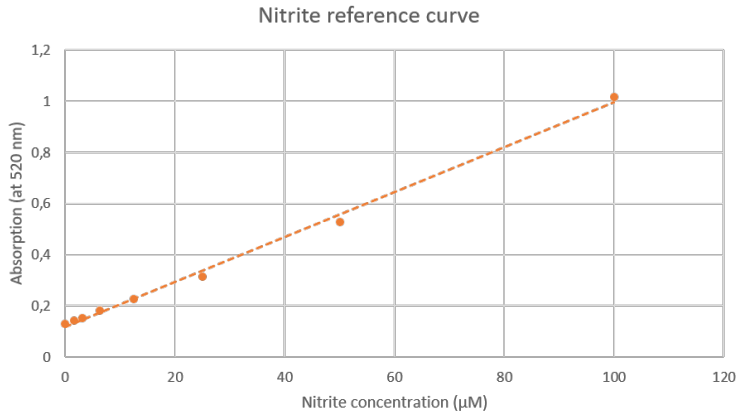

Figure 5: Graph of the nitrite reference curve of Day 6, with fixed concentrations. 0, 1.56, 3.13, 6.25, 12.5, 25, 50 and 100 µM are the known concentrations, which are measured on their absorbance of 520 nm light in a plate reader.

Immunofluorescence analysis

As for the qPCR samples, medium was removed and channels were washed with PBS. Cells were fixated by adding 4% paraformaldehyde 0.1M in 1x PBS twice in the channels of the sample for 15 minutes. After fixation, cells were washed with PBS three times. Cells were incubated in a permealization buffer (0,25% Triton-X in 1x PBS) for 10 minutes at room temperature. Cells were again washed with 1x PBS 3 times. Blocking solution (1% BSA in 1x PBS) was added to the samples and incubated for 20 minutes at room temperature. Cells were washed again 3 times with PBS and primary antibodies (stated in table 1) were added to the samples, incubated overnight at 4°C. After incubation, cells were washed with 1x PBS three times and secondary antibodies were added next, incubated for 1 hour at room temperature in the dark. Cells were washed with 1x PBS three times and 0,1 µg/mL DAPI is added to the cells, incubated for 5 to 10 minutes at room temperature in the dark. At last, cells were washed thrice with 1x PBS. Samples were stored wrapped in a parafilm in a petridish, in the dark at 4°C prior to analyzing with the NIKON Confocal Laser Microscope A1 (Nikon Instruments, the Netherlands). Images were then analyzed and processed with Fiji (Fiji, USA). For CD163 staining, cells were counted with sufficient staining of CD163, using Microsoft Paint (USA) and a counter. Next to this, DAPI stained nuclei were counted too to calculate a ratio of CD163 positive macrophage. The following formula is used to calculate the described ratio:

$$CD163^{+}/DAPI^{+} = countedCD163positivecells/countedDAPIstainednuclei$$

The primary and secondary antibodies that were used in this report are presented in table 1 and 2.

Target	Primary antibody	Used in chamber	Dilution	Source
Collagen I	Rabbit anti-Collagen I	Top chamber	1:100	Abcam
Collagen VI	Rabbit anti-Collagen VI	Top chamber	1:200	Abcam
HAS-1	Mouse anti-Hyaluronansynthase 1	Top chamber	1:200	Abcam
CD163	Rabbit anti-CD163	Top chamber	1:50	Abcam
CD80	Mouse anti-CD80	Top chamber	1:200	Abcam
CD68	Mouse anti-CD68	Top chamber	1:100	Abcam
VECadherin	Mouse anti-VECadherin	Bottom chamber	1:100	Abcam

Table 1: Primary antibodies used with their dilution and source.

Secondary antibody	Used in chamber	Dilution	Source
Alexa Fluor 565 Phalloidin	Top and bottom chamber	1:400	Abcam
Alexa Fluor 488 donkey anti-rabbit	Top chamber	1:250	Abcam
Alexa Fluor 488 donkey anti-mouse	Top and bottom chamber	1:200	Abcam
Alexa Fluor 647 donkey anti-mouse	Top chamber	1:200	Abcam
DAPI	Top and bottom chamber	1:100	Abcam

Table 2: Secondary antibodies used with their dilution and source.

qPCR analysis
Media was removed and the systems were washed one time with PBS. 50 µL of qPCR lysis buffer (Qiagen, Germany) was added to the top chamber twice. The buffer was sucked up and added to a 2 ml Eppendorf tube. Another 250 µL of qPCR lysis buffer was added to the same Eppendorf tube. After the samples were collected, the samples were stored at -30 °C. Ribonucleic acid (RNA) of the samples was isolated from the samples using the RNeasy Mini Kit (Qiagen 74107, Germany) as described by the manufacturer. Concentration of RNA in the samples was determined using the Nanodrop 2000 spectrophotometer (Thermo Scientific, the Netherlands). Complementary DNA (cDNA) was created from the RNA samples by adding 4 µL iScript (Bio-rad, USA) and 1 µL Reverse Transcriptase (Bio-rad, USA) to the sample. Samples were then runned through a predescribed program in the Bio-Rad CFX Connect Real-time system (Bio-rad, USA).

cDNA was diluted to a concentration of 5 ng/8 µL by adding RNase-free water. Primers were prepared by combining both equal amounts of forward and reverse versions of the primer. As a housekeeping gene, *GAPDH* was selected to normalize the values. For analysis and functionality of the human synovial fibroblasts seeded, *COL1A1*, *Col6A1* and *HAS1* were used as primers. For analysis and study of the polarization to M1 macrophages, *CD80*, *IL1R* and *iNOS* were selected as primers. For the study of M2 polarization and its subgroups, *CD163*, *CD200R*, *SPHK1*, *TLR1*, *TLR8* and *IL10* were used. First, 10 µL SYBR Green Reagent (Sensimix Bioline Reagents, UK) was added into a 384 wells plate. Next, 2 µL of forward and reverse mixes of each primer were added to the 384 wells plate, with each row resembling a new primer set. Lastly, 8 µL diluted cDNA samples were added with each column representing a new cDNA dilution. Ct values of the samples were gathered by using the Bio-Rad CFX Connect Real-Time system (Bio-Rad, USA). Ct values of the selected primers were normalized by substracting the Ct values from the housekeeping gene. These so-called ΔCt values were then further calculated by the following formula: $2^{-\Delta Ct}$. These $2^{-\Delta Ct}$ values were multiplied by 100, analyzed in Microsoft Origin (USA). Values higher than 1000 were excluded from the data set, as well as data points that were 8 times higher than the second highest value.

Outline of the project
An overview is given in figure 6, where is shown what is done on which day. As shown, the systems are first prepared, prior to seeding of synovial fibroblasts and HUVEC seeding. Macrophages are seeded on day 5 and on day 6, 8 and 10 results are gathered.

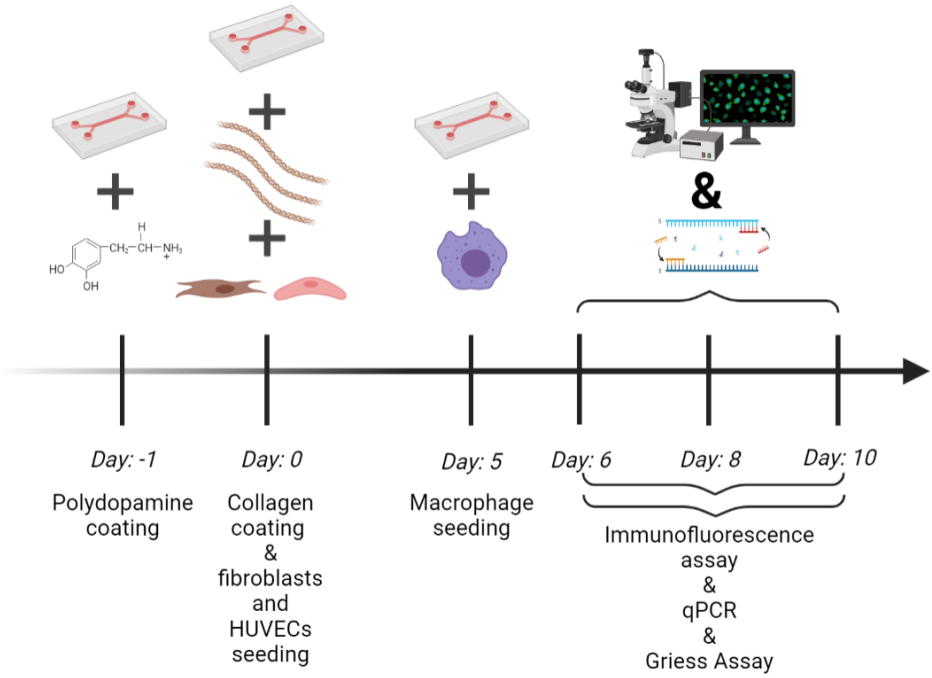

Figure 6: The outline of the project, described for all days. Day 0 is assumed as the day that the first cells are seeded.

In this report, three distinctive conditions will be discussed and analyzed:

1. Samples seeded with only human synovial fibroblasts seeded in the top compartment of the system. This condition will be called '**single culture**' for the rest of the report.

2. Samples seeded with both human synovial fibroblasts and macrophages seeded in the top compartment. This condition will be called '**double culture**' for the rest of the report.

3. Samples seeded with human synovial fibroblasts, macrophages seeded in the top compartment and HUVEC cells seeded in the bottom compartment of the system. This condition will be called '**triple culture**' for the rest of the report.

3 Results

In this section, an analysis is shown of the data that had been retrieved from our samples. Samples were seeded as discussed in section 2. The samples were first analyzed with transmission light microscopy. Next, the quantitative data of NO using the Griess Kit is presented. Furthermore, immunofluorescence data is shown to analyze the samples in a qualitative manner. Lastly, qPCR analysis is presented, which provides a quantitative analysis of macrophage polarization and extracellular matrix elements.

3.1 Cell Seeding

To determine whether the cells would integrate on the collagen I layer in the channels, human synovial fibroblasts were studied in the system for 7 days. As can be seen in figure 7 below, cells were successfully seeded in the top compartment. Figure 7a shows a schematic view of the sample viewed from the top. As can be seen in figure 7, the top left channel shows no cells in it whereas the bottom left channel present a dense cluster of fibroblast cells. An identical view can be seen in figure 7b with no cell structure in the top left channel and a high density of cells in the bottom left channel. A rough cell structure is seen on day 3 (figure 7b), which becomes smoother over the days. This results in a smooth cell structure seen on day 7 (figure 7d), which suggests complete integration of the fibroblast in the collagen I layer.

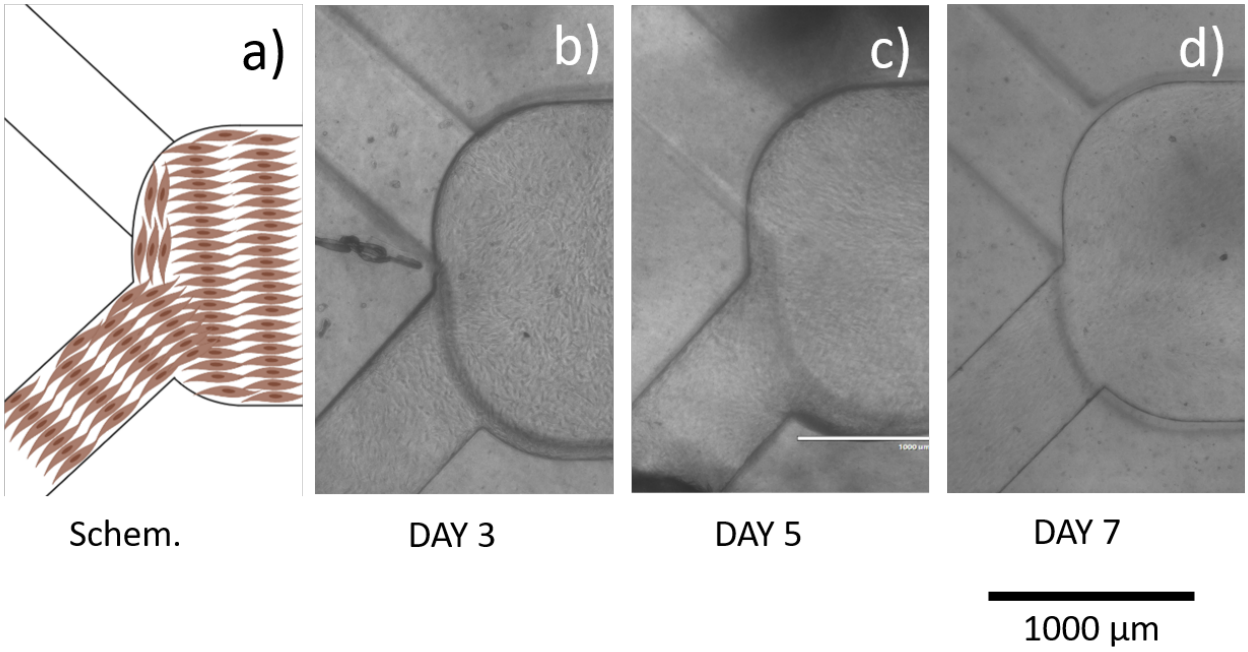

Figure 7: Top view of top compartment of the system, seeded with human synovial fibroblasts 4x. a) Schematic view of cell seeding, with an empty bottom chamber (no cells in top left channel) and fibroblast cells in the bottom left channel and chamber. Figure 7a is made in BioRender. b) c) and d) show human synovial fibroblasts seeded in top compartment on respectively day 3, 5 and 7. Top left channel is empty as no cell structures are visible Figures are made with EVOS transmission microscope (Thermofisher, USA). Scale bar: 1000 µm

On day 5 of the experiment, 3 hours after the macrophages were seeded, images were taken of both the double and the triple culture condition. In figure 8a, the double culture is shown with red boxes surrounding clusters black dots. Black dots represented macrophages that were poorly integrated into the system. In figure 8b, the triple culture condition is shown with fewer red boxes surrounding the spotted black dots on the image. For both images, a rough cell structure of synovial fibroblasts is still visible around the clusters of macrophages.

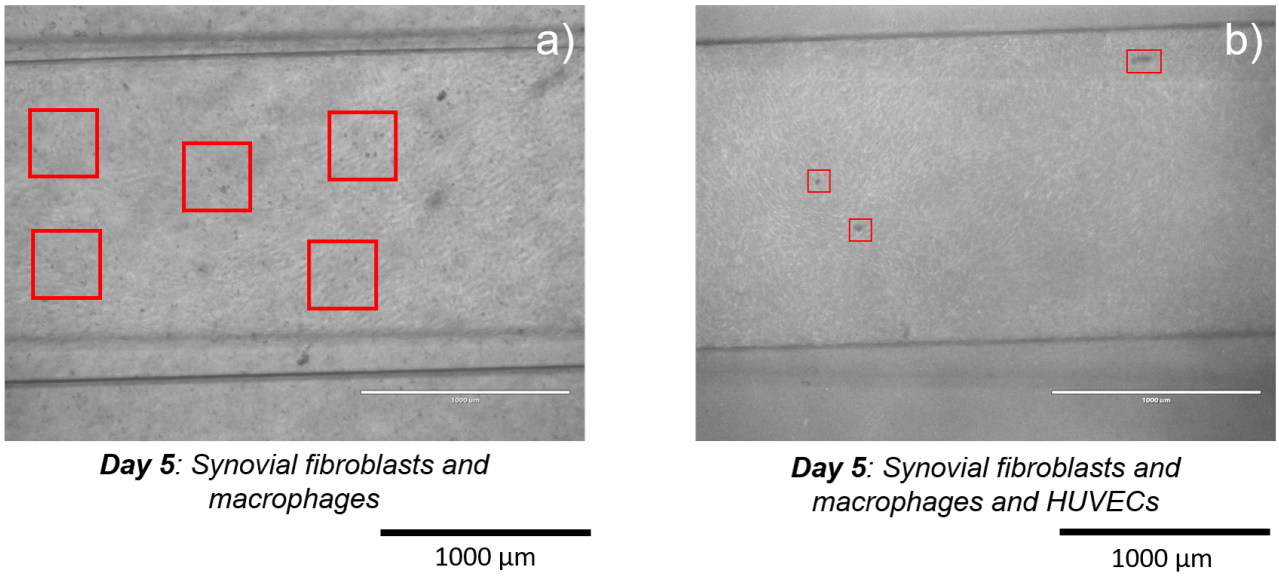

Figure 8: Top view of top compartment of the system, seeded with human synovial fibroblasts and macrophages 4x. Red boxes representing clusters of poorly integrated macrophages in the system a) Double culture sample. b) Triple culture sample. Scale bar: 1000 µm

Figure 9 shows figure 8a zoomed in at 10x. When zoomed in, the black dots become a lighter colour as shown with the red arrow. Both black dots and lighter circles present poorly integrated macrophages.

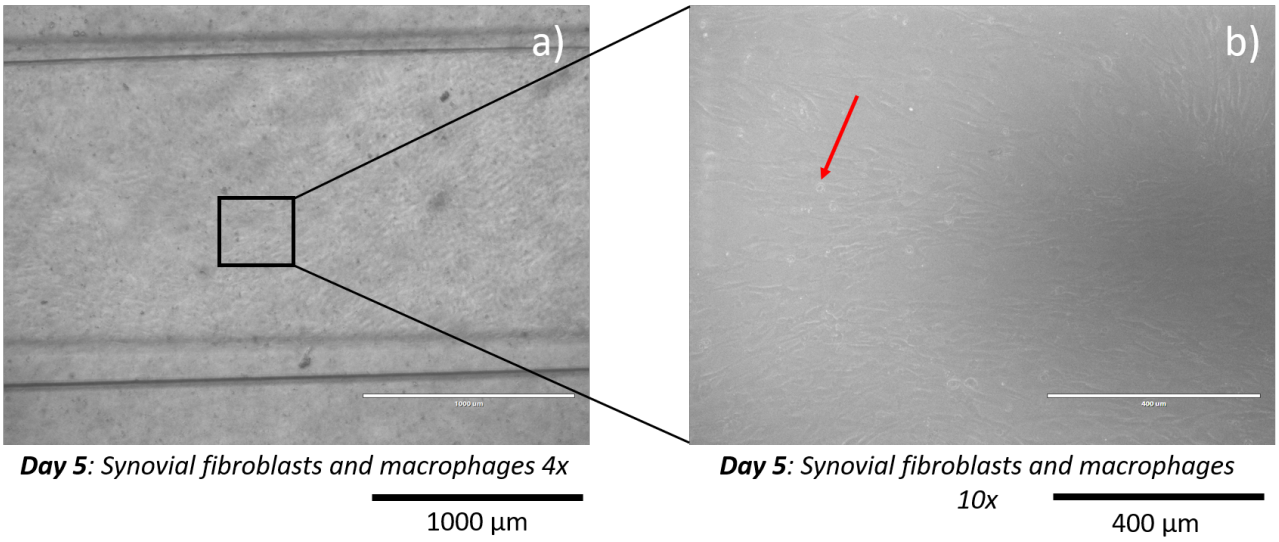

Figure 9: Top view of the top compartment of the system, seeded with human synovial fibroblasts and macrophages. a) Middle of the sample b) zoomed in on part indicated by a black square in a) Red arrow shows example of partially integrated macrophage in the system, representing a lighter circle. Scale bar at a): 1000 µm, scale bar at b) 400 µm

Figure 10 shows a combination of both double and triple culture, for day 5, 7 and 10. Without HUVECs in the bottom chamber, macrophages are more visible as black dots. On day 7, major clusters of macrophages are visible for double culture samples. On day 10, visible macrophages are spread out across the sample, with a few small clusters still visible. For the triple culture samples, macrophages were less visible and became even less visible in the measured period.

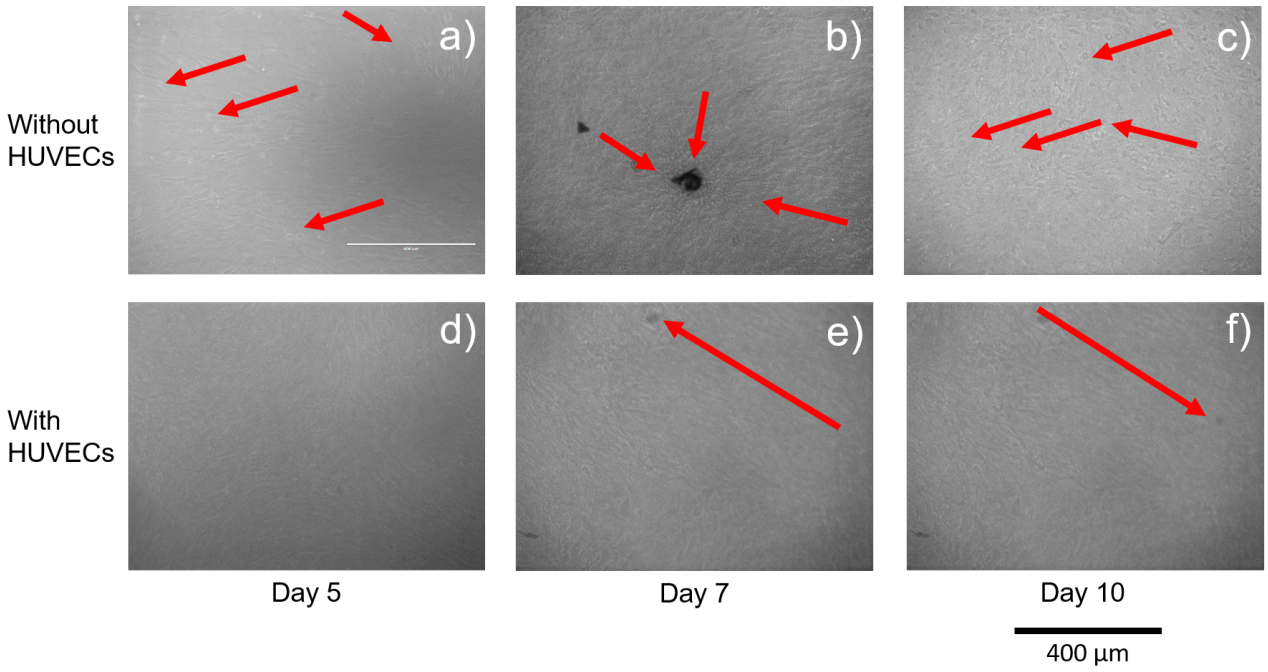

Figure 10: Top view of the synovial membrane-on-chip showing the synovial fibroblast and macrophages layer for both double and triple culture at day 5, 7 and 10. 20x a), b) and c) representing double culture samples and d), e) and f) representing triple culture samples. a) and d) representing day 5, b) and e) representing day 7 and c) and f) representing day 10 of the experiment. Red arrows present poorly integrated macrophages. Scale bar: 400 µm

3.2 Griess Assay

The Griess Kit was used as described in section 2, *Griess assay*. Differences in absorbance could be seen between the chosen conditions. A minor difference of nitrite concentration was found at day 6 between the samples without (32,517 ± 7,278 µM) and with HUVECs (24,148 ± 1,091 µM). An increase in nitrite concentration was detected at day 8 for the samples without HUVECs (64,018 ± 12,741 µM) suggesting an increase in NO production in double culture samples. Interestingly, while the nitrate concentration remained similar at day 10 for the samples without the HUVECs, it drastically decreased for the samples with HUVECs (2,507 µM).

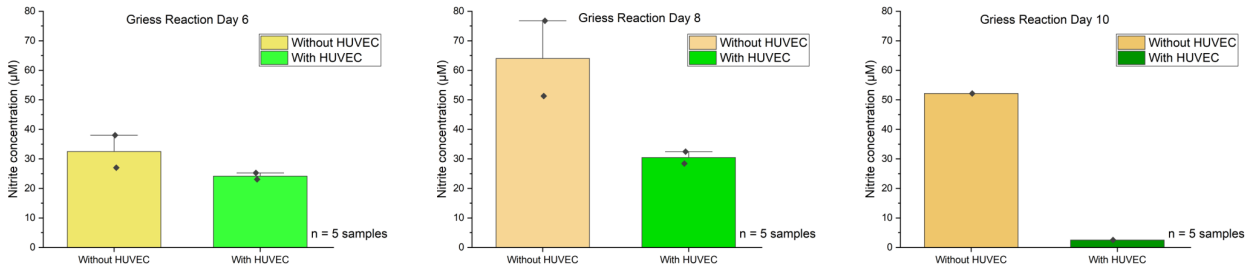

Figure 11: Graphs presenting the nitrite concentrations in µM of the samples with and without HUVECs at on day 6, 8 and 10. Black dots represent the measurement of 5 samples combined and positive error bars are shown by black T-like lines. Y-axis is at the same level for each graph.

3.3 Immunofluorescence

3.3.1 Collagen production

Collagen I production of synovial fibroblasts increased progressively the longer the culture. At day 3 (figure 12a) and 6 (figure 12b)) low collagen I staining was detected, while a fiber-like web can be noticed at day 10 (figure 12c) suggesting an increase in protein production. Moreover, increased number of nuclei could be seen

at different days suggesting not only extracellular matrix (ECM) production, but also high proliferation. The sample of day 3, counted 160 nuclei. Day 6 counted 219 nuclei, while day 10 counted 516 nuclei suggesting higher proliferation between day 6 and day 10.

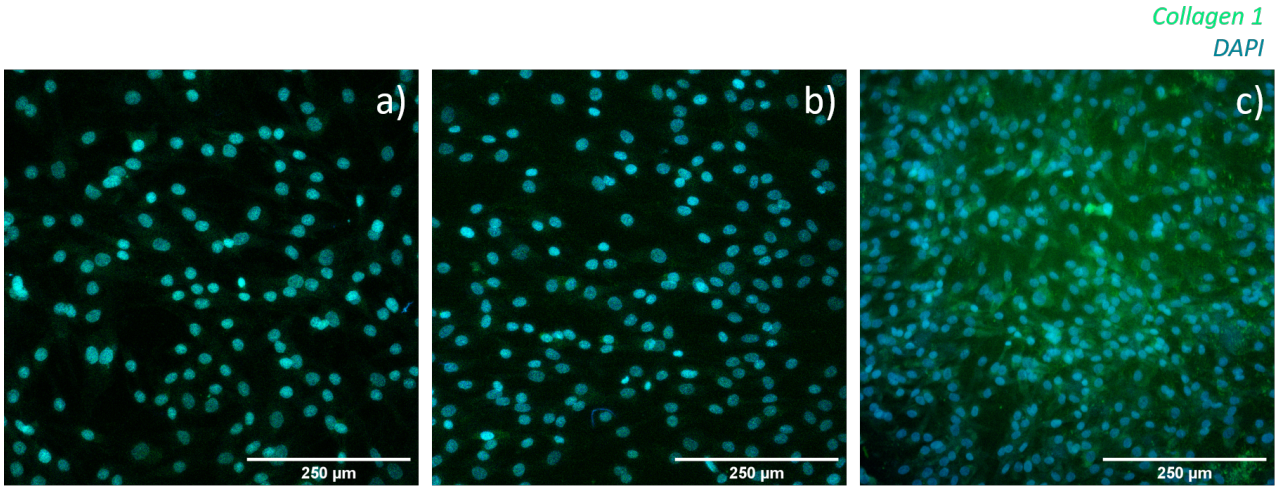

Figure 12: Top view of the synovial fibroblast layer with collagen I (in green) and DAPI (in blue). a) day 3 b) day 6 c) day 10. Scale bar: 250 µm

Triple culture samples on day 6 showed fibers of collagen I (figure 13). Heterogeneity is visible in both zoomed and not zoomed pictures. Compared to collagen I production for synovial fibroblasts on day 6 in figure 12b, the triple culture samples showed more collagen I staining, suggesting higher ECM production.

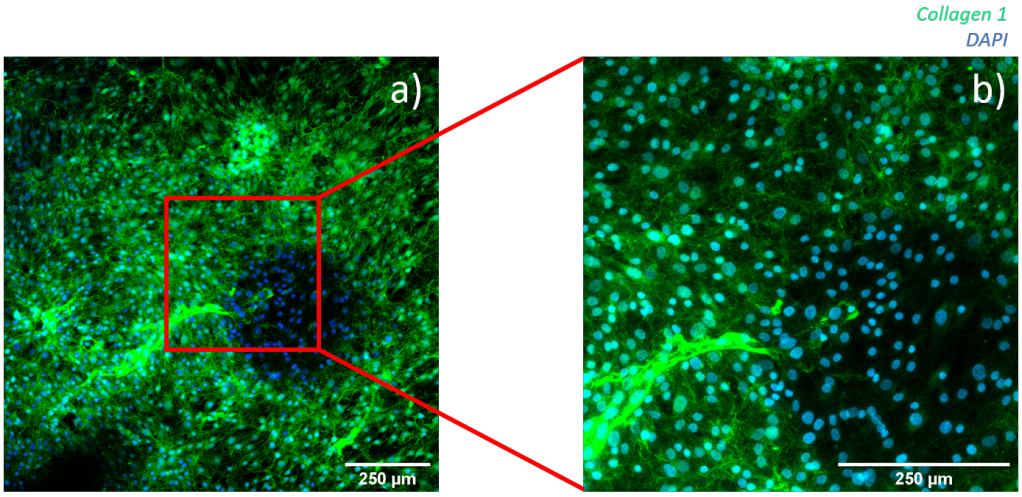

Figure 13: Top view of the synovial fibroblast layer for a triple culture sample with collagen I (in green) and DAPI (in blue), zoomed in on section shown in red. Scale bar: 250 µm

For double culture samples (figure 14a), collagen I staining showed the extracellular matrix of the coculture in the synovial fibroblasts and macrophage layer. Triple culture samples (figure 14b) showed a heterogeneous accentuation of collagen I. Clusters of collagen I were visible in triple culture samples, whilst no collagen I clusters were visible in double culture samples. Moreover, voids visible on day 6 for triple culture samples in figure 13a were less visible on day 10 in figure 14.

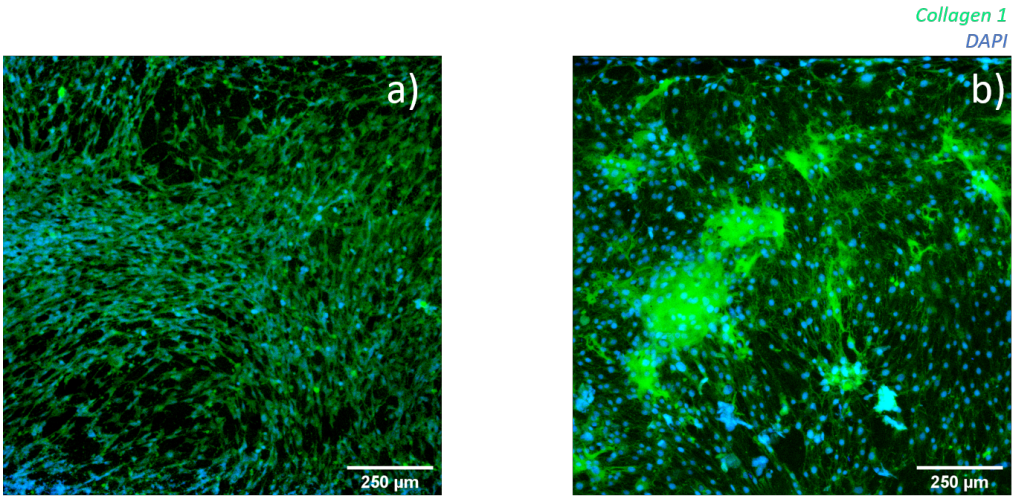

Figure 14: Top view of the synovial fibroblast and macrophage layer with collagen I (in green) and DAPI (in blue). a) Double culture sample b) Triple culture samples. Scale bar: 250 µm

3.3.2 HAS1

HAS1 production of synovial fibroblasts cocultured with macrophages showed high signal on day 10 for double culture samples. Compared to signal of collagen I in figure 12, HAS1 signal in figure 15 was higher on day 10 than the collagen I signal. HAS1 seemed to stain the cytoplasma of the cells. This suggests that HAS1 is a potential marker for synovial fibroblasts. DAPI stained aspecific, resulting in unreliable signal.

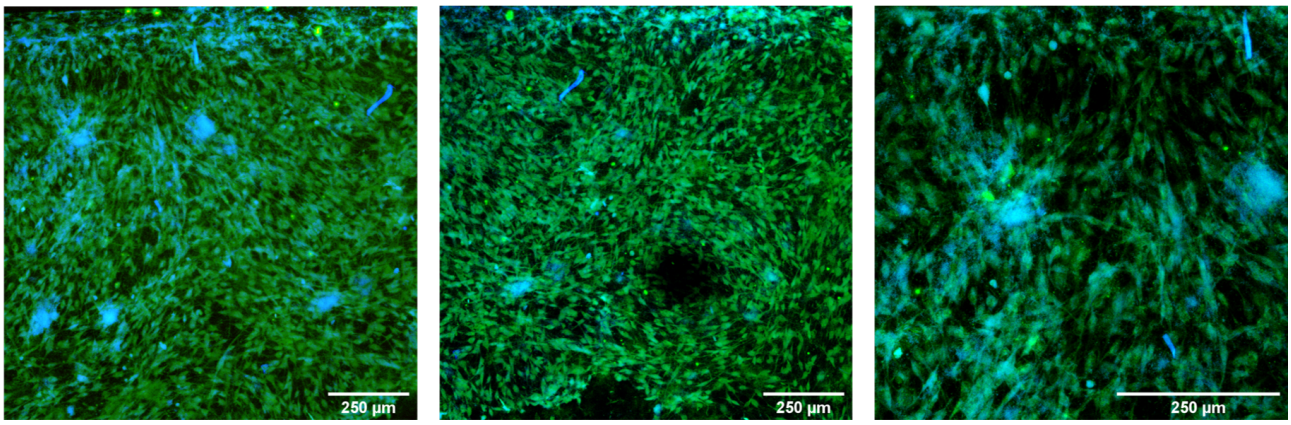

Figure 15: Top view of the synovial fibroblast and macrophage layer with HAS1 (in green) and DAPI (in blue) of double culture samples on day 10. Scale bar: 250 µm

3.3.3 CD163 and CD80

Triple culture samples showed higher CD163 signal, than double culture samples. Double culture samples on day 6 had 18 CD163 positive cells and 252 DAPI stained nuclei, showed in figure 16a. The double culture sample on day 6 had a ratio of 0,0714 $CD163^+/DAPI^+$. Double culture sample on day 10 had 23 CD163 positive cells and 436 DAPI stained nuclei, showed in figure 16b. The double culture sample on day 10 had a ratio of 0,0528 $CD163^+/DAPI^+$. Triple culture sample on day 6 had 82 CD163 positive cells and 875 DAPI stained nuclei, showed in figure 16c. The triple culture sample on day 6 had a ratio of 0,0937 $CD163^+/DAPI^+$. Triple culture sample on day 10 had 58 CD163 positive cells and 441 DAPI stained nuclei, showed in figure 16d. The triple culture sample on day 10 had a ratio of 0,1312 $CD163^+/DAPI^+$. Moreover, increased number of nuclei could be seen at different days suggesting not only a difference in amount of CD163 positive macrophages, but also difference in proliferation. While triple culture samples showed a decrease in cells, double culture samples showed substantial proliferation. CD80 signal was not visible in any of the samples.

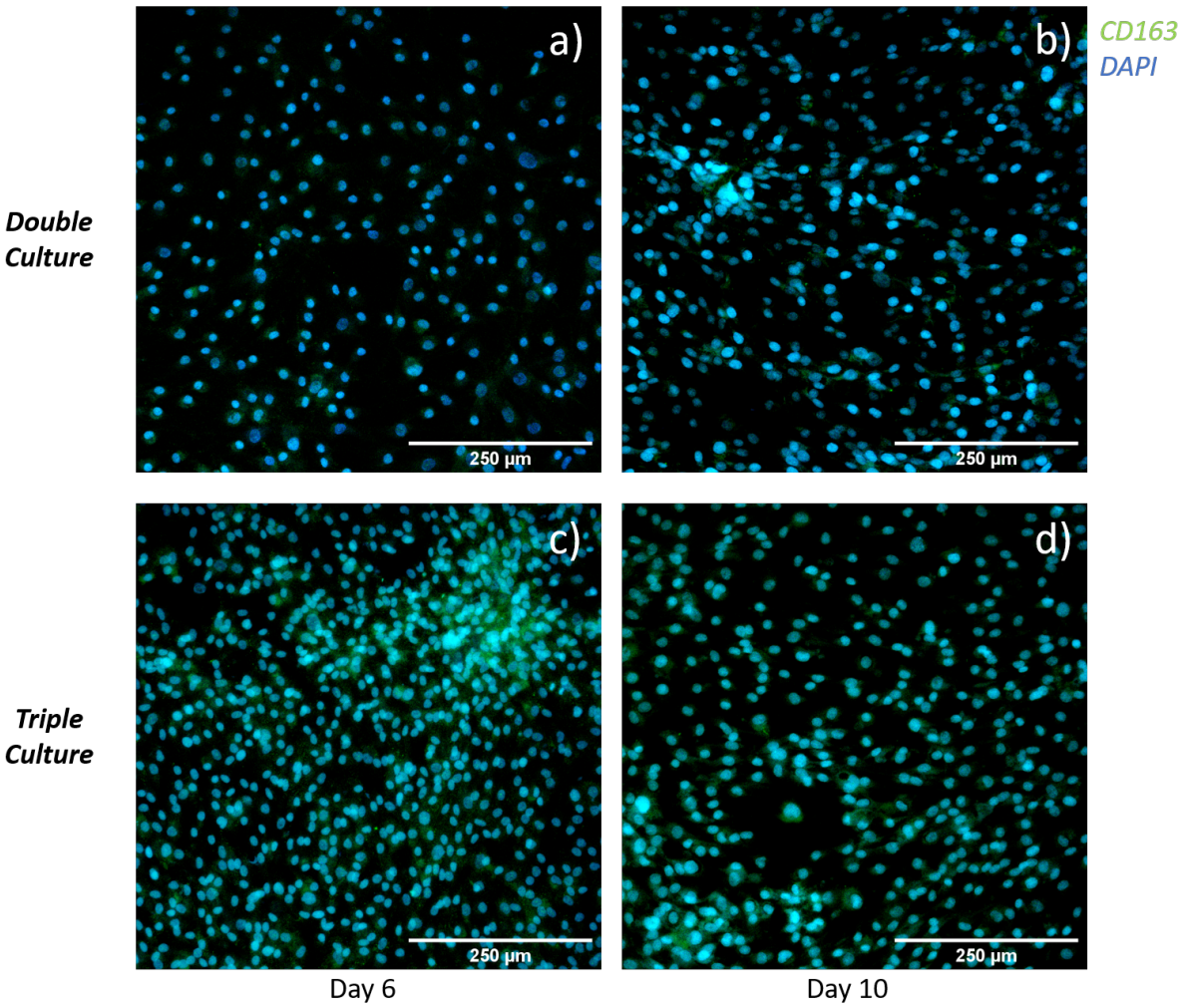

Figure 16: Top view of the synovial fibroblast and macrophage layer with CD163 (in green) and DAPI (in blue) staining, 20x. a) and c) Double culture samples, day 6 and day 10 respectively. b) and d) Triple culture samples, day 6 and day 10 respectively. Scale bar: 250 µm

3.3.4 HUVECs

On day 6 (figure 17a and 17c), the area of the cells given by Phalloidin seemed to be larger, with respect to day 10 (figure 17b and 17d). Moreover, the HUVEC layer seemed to partially cover the surface at day 6, while at day 10 the cells looked packed. VE-cadherin signals seem to be brighter on day 6, than day 10. This suggests that the HUVECs at day 10 are tightly packed. Furthermore, the complete cover of the channel with HUVECs at day 10 respect to day 6 suggests proliferative activity.

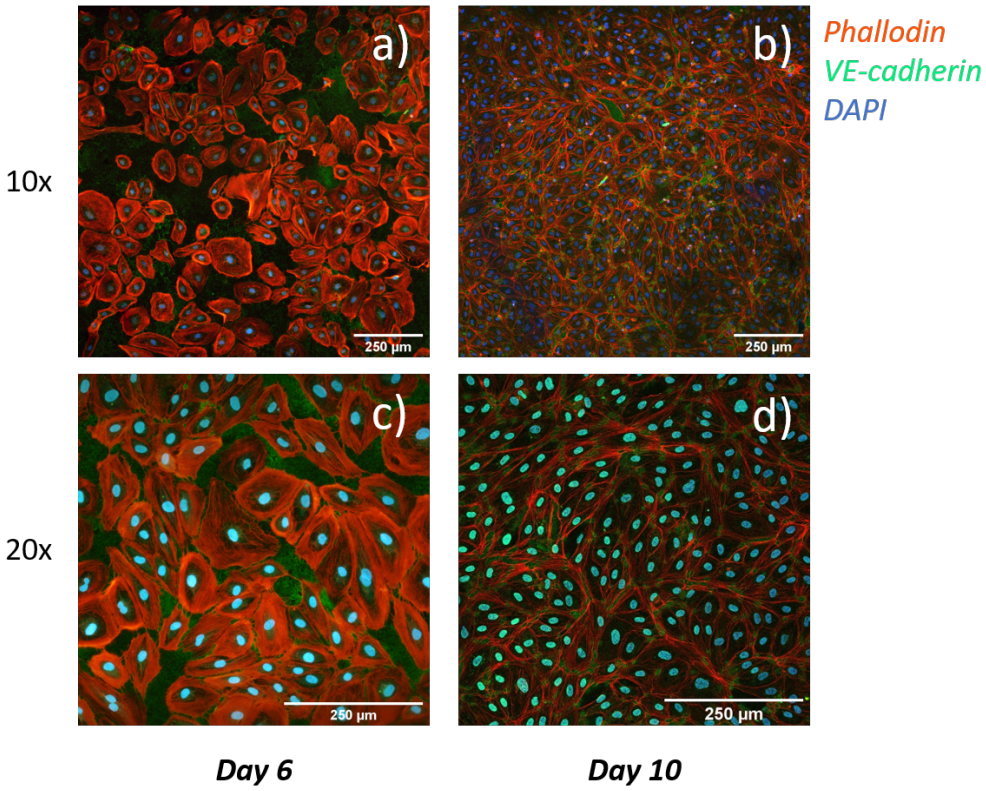

Figure 17: Top view of the HUVEC layer with Phalloidin (in red) VE-cadherin (in green) and DAPI (in blue) staining a) and b) represent 10x magnification, while c) and d) represent 20x magnification. HUVEC cells on day 6 are shown in a) and c), while b) and d) show images taken on day 10 of HUVEC cells. Scale bar: 250 µm.

3.4 qPCR

In blue, data of single culture samples is shown. In yellow or orange, data of double culture samples in the top compartment of the system (double culture) is shown. In green, data of double culture with HUVEC cells in the bottom compartment (triple culture) is shown. A lighter shade of the colour represents day 6 of the experiment, referred to the outline of the project as shown in figure 6. A darker shade of the colour represents day 10 of the experiment is shown.

3.4.1 Gene expression of *COL1A1*

Collagen I (*COL1A1*), an anabolic gene, seemed to decrease in relative gene expression on day 10 of the experiment with respect to day 6 for all conditions (figure 18). A high increase in gene expression was found in the so-called double culture on day 6, whereas it seemed that *COL1A1* gene expression is minimized on day 10 of the double culture samples. Higher expression of *COL1A1* was seen in double culture samples, than triple culture samples.The *COL1A1* gene appeared to be expressed in a lower quantity on day 10 of the triple culture samples, than double culture samples. Whilst double culture samples on day 6 had higher expression of *COL1A1* and triple cultures had a lower expression on day 6 than the single cultures, *COL1A1* of both double and triple cultures was lower expressed on day 10 than single cultures.

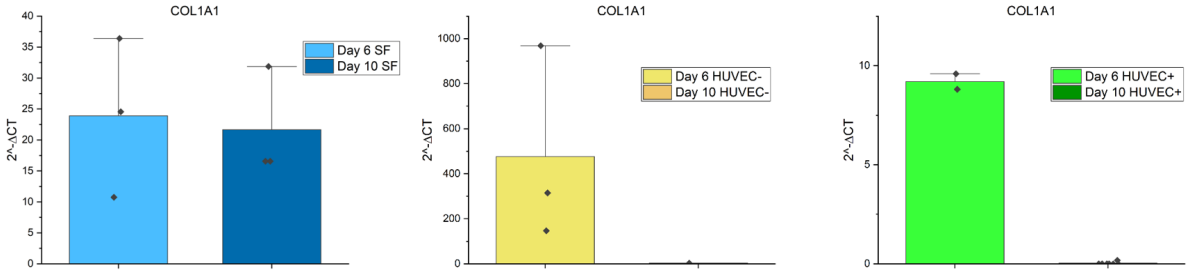

Figure 18: Relative gene expression of COL1A1. This marker showed the behaviour of the ECM in the top compartment of the system. qPCR data of the single culture is shown in blue. qPCR data of the double culture is shown in yellow or orange. qPCR data of the triple culture is shown in green. A light shade of the colour used is day 6, whereas a darker shade represents day 10 of the experiment. Black dots represent data points and positive error bars are shown by black T-like lines. Y-axis is not at the same level for each graph.

3.4.2 Gene expression of *COL6A1* and *HAS1*

Relative gene expression of *COL6A1* and *HAS1* is shown in figure 19. The primers chosen and analyzed in figure 19 present the behaviour of human synovial fibroblasts seeded in the top compartment of the system and its extracellular matrix for *COL6A1*. Also, *COL6A1* presents the extracellular matrix around the cells. The *COL6A1* gene expression appeared to increase on day 10 with respect to day 6 for single culture samples. For double culture samples, an increase on day 10 with respect to day 6 was again found, with a significantly lower gene expression of *COL6A1* on day 6 with respect to the single culture samples on day 6 and 10 of the experiment. *COL6A1* gene expression remained consistent for triple culture samples, considering day 6 and day 10 of the experiment.

HAS1 gene expression appeared to be consistent for all conditions. It could be seen that *HAS1* gene expression decreased on day 10 with respect to day 6 for all cultures. It may, however, be debated if this is true as error bars are considerably large for all conditions. These large standard deviations suggest a difference of *HAS1* gene expression between samples of the same condition.

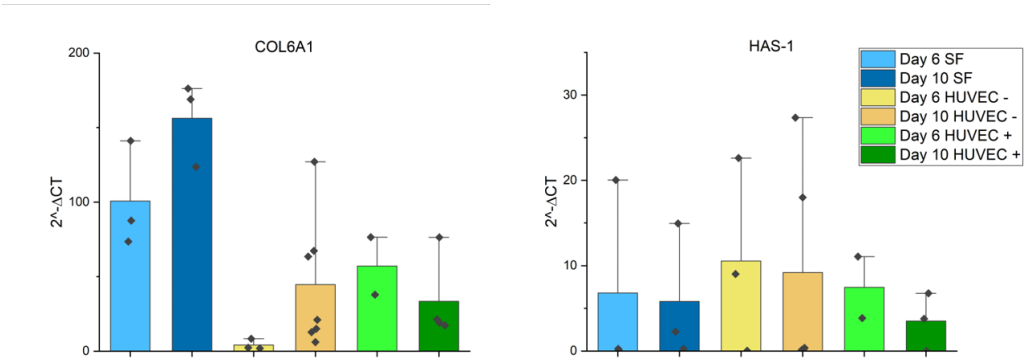

Figure 19: Relative gene expression of synovial fibroblast markers COL6A1 and HAS1. These markers showed the behaviour of the human synovial fibroblasts in the top compartment of the system. qPCR data of the single culture is shown in blue. qPCR data of the double culture is shown in yellow or orange. qPCR data of the triple culture is shown in green. A light shade of the colour used is day 6, whereas a darker shade represents day 10 of the experiment. Black dots represent data points and positive error bars are shown by black T-like lines. Y-axis is not at the same level for each graph.

3.4.3 Gene expression of M1 markers

Relative gene expression of *IL1R*, *CD80* and *iNOS* is shown in figure 20. The primers chosen and analyzed in figure 20 present the relative abundance of M1 polarized macrophages. The gene expression of *IL1R*, a receptor for the cytokine interleukin 1, is abundant in M1 macrophages. For single culture samples, where only synovial fibroblasts are seeded in the top compartment of the system, *IL1R* gene expression increased on day 10 with respect to day 6. Comparable changes in gene expression was seen in double culture samples, with less gene expression for day 6 double culture samples than day 6 synovial fibroblasts only samples. Dissimilar results appeared for triple culture results, as *IL1R* gene expression was reduced significantly on day 10 with respect to day 6. *IL1R* gene expression for day 6 seeded with HUVEC cells was, however, higher than samples on day 6 not seeded with HUVECs.

Gene expression of the gene *CD80* corresponds mostly to macrophages polarized to M1 macrophages. Clearly, single culture samples showed very little gene expression of *CD80* for both day 6 and day 10. Day 6 for both double and triple culture samples again showed very little gene expression of *CD80*. Day 10 of both double culture and triple culture samples showed an increase of *CD80* gene expression with respect to day 6 of both conditions. Triple culture samples on day 10 showed a higher gene expression of *CD80*, than double culutre samples on day 10.

As a quantitative analysis of NO was done with the Griess Kit described in section 3.2, a quantitative analysis with qPCR was done for one of the forms of nitric oxide synthase; inducible nitric oxide synthase (*iNOS*). This synthase is mostly abundant in M1 macrophages, which makes it a potential marker for study of polarization to a M1 macrophage. For synovial fibroblasts seeded only samples, *iNOS* gene expression was low when compared to double and triple culture samples. This suggests no iNOS production of synovial fibroblasts. An increase in expression is seen for double culture samples on day 10, suggesting higher production of NO. As can be seen in section 3.2, high levels of NO were seen on day 10 with higher levels of NO, compared to day 6. Less iNOS is expressed for triple culture samples than double culture samples on day 6. A high increase is seen on day 10 for triple culture samples. This is not in line with the data retrieved from the Griess assay (section 3.2).

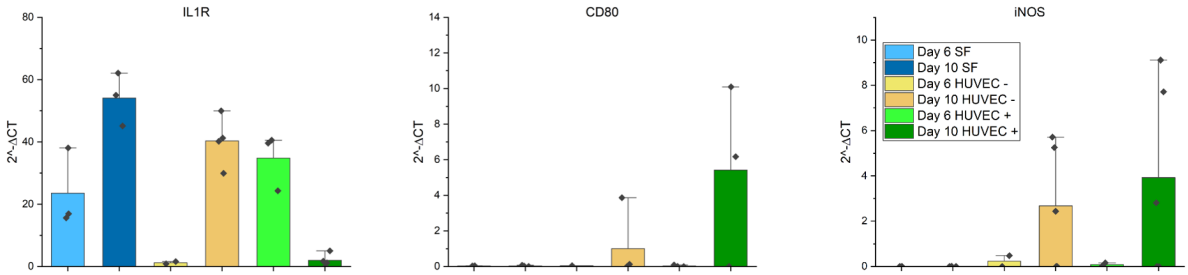

Figure 20: Relative gene expression of used M1 markers, IL1R, CD80 and iNOS. These markers show the behaviour in polarization of macrophages to a M1 state in the top compartment of the system. qPCR data of the single culture is shown in blue (SF is synovial fibroblasts only). qPCR data of the double culture is shown in yellow or orange. qPCR data of the triple culture is shown in green. A light shade of the colour used is day 6, whereas a darker shade represents day 10 of the experiment. Black dots represent data points and positive error bars are shown by black T-like lines. Y-axis is not at the same level for each graph.

3.4.4 Gene expression of M2 markers

Relative gene expression of *CD163*, *SPHK1* and *TLR1* are shown in figure 21. The primers chosen and analyzed in figure 21 present the relative abundance of M2 polarized macrophages. Gene expression of Cluster of Differentiation 163 (*CD163*) is mostly abundant in M2a and M2c subgroups of polarized macrophages. For single culture samples, gene expression of *CD163* was low on both days with respect to other conditions. For double culture samples, an increase was seen in gene expression on day 10 with respect to day 6. Moreover, a

considerable difference was seen in the triple culture samples. A substantial expression of the *CD163* gene was seen on day 10 with respect to day 6 for triple culture samples.

Gene expression for Sphingosine Kinase 1 (*SPHK1*) presents the abundance of M2b subgroup macrophages, which indicates polarization to M2 macrophages. For single culture samples, a low expression of *SPHK1* was seen with a decrease on day 10. For double culture samples, a high expression of *SPHK1* was seen on day 6. Double culture samples presented a decreased expression of *SPHK1* on day 10 to the level of single culture samples. Samples with HUVECs showed an increase on day 10 with respect to day 6. The expression of triple culture samples on day 10 seemed to be lower, than the expression of double culture samples on day 6.

Gene expression for Toll-like receptor 1 presents the abundance of M2c subgroup macrophages, which indicates polarization to M2 macrophages. For single culture samples, low gene expression could be found for *TLR1*. *TLR1* expression seemed to increase on day 10 with respect to day 6, with a low expression on day 6. For triple culture samples, high expression was seen between on day 10 with a low expression seen on day 6 for *TLR1*.

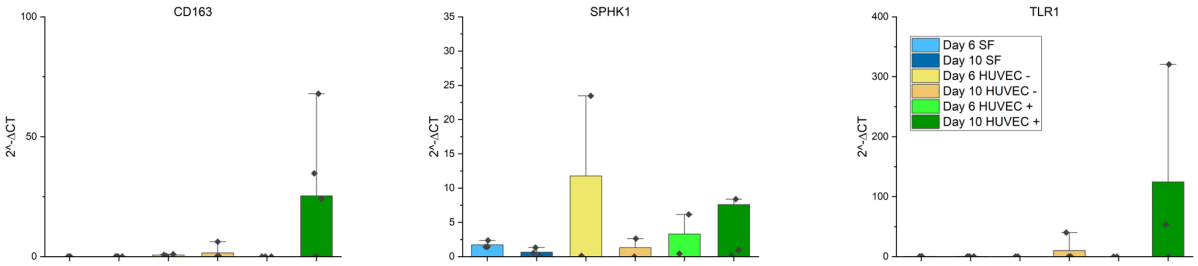

Figure 21: Relative gene expression of M2 markers CD163, SPHK1 and TLR1. These markers show the behaviour in polarization of macrophages to a M2 state in the top compartment of the sample. CD163 represents macrophages that polarize to a M2a state, SPHK1 represents M2b and TLR1 represents M2c. qPCR data of the single culture is shown in blue. qPCR data of the double culture is shown in yellow or orange. qPCR data of the triple culture is shown in green. A light shade of the colour used is day 6, whereas a darker shade represents day 10 of the experiment. Black dots represent data points and positive error bars are shown by black T-like lines. Y-axis is not at the same level for each graph.

4 Discussion

4.1 Cell seeding

Black dots in 8a and grey round elements, as previously presented (the red arrow in 8b), present poor integrated macrophages in the system and in the human synovial fibroblasts. It is assumed that poorly integrated macrophages represent M1 macrophages. During inflammation, M1 macrophages tend to move to the inflamed area and act on this inflamed area [43] [44]. Migration of macrophages could be the reason why macrophages are poorly integrated [44]. If this is assumed and more macrophages are poorly integrated for the double culture than the triple culture samples, this means that inflammation is initiated in double culture samples. An inflammation in the double culture could state that macrophages are more prone to a M1 state of macrophage, as this macrophage has a pro-inflammatory function [23]. Also, this poor integration gets worse during the experiment, which then should indicate that there are more pro-inflammatory (M1) macrophages in the double culture samples.

4.2 Griess Assay

Production of NO is mainly caused by NOS, which exists in 3 distinctive forms. As qPCR analysis is done of only *iNOS*, analysis of other NOS forms should be taken into consideration in future experiments. This could provide an indication of which cells cause production of NO and thus which cells cause an increase in the concentration of NO. As research has shown [45], eNOS is an important form of NOS that could potentially trigger inflammation. Endothelial cells, which include HUVEC cells used in our experiment, mainly express this gene. The NO produced by the HUVECs in the bottom compartment, however, cannot diffuse through the PDMS membrane in between the system as NO only has a very short halflife. On day 8, a stable concentration of NO is formed for the double culture. Day 10 of double culture samples presents a condition with a high concentration of NO, while day 10 of triple culture samples presents a condition with a low concentration of NO.

Chemicals such as a nitric oxide inhibitor or donor can be used to control the effect of nitric oxide. Due to a lack of time, this could not be done in this thesis. An example of an inhibitor is L-NMMA [33]. This molecule blocks the synthesis of nitric oxide by blocking all forms of nitric oxide. With such a molecule, the effect of no nitric oxide can be measured to the cells. Moreover, iNOS specific inhibitors such as 1400W [31], [45] can be used to study the effect of eNOS specifically on the polarization of macrophages. Last, a NO-donor can be used to study the effect of an artificial high nitric oxide concentration. It has been proven that an increase in SNAP concentration leads to an increase of TNF-α [36]. As TNF-α is a M1 marker, high NO concentrations seem to lead to polarization to M1 macrophages. Using L-NMMA or SNAP might give even more insights in the effect of nitric oxide on macrophage polarization in the synovial membrane.

4.3 Immunofluorescence

In figure 12, an increase is seen in collagen I. This increase is clearly due to the synovial fibroblasts, as these are the only cells seeded in this condition. What can be seen too, is a different increase of collagen I in samples of the triple culture on day 10. Large clusters and fibers of collagen I are visible on day 10 (figure 14b). For double culture samples, clusters of collagen I are not visible (figure 14a). In section 1.3 is stated that M2 macrophages are tissue regenerative. As collagen I is a critical ECM element in tissue, a higher production of collagen I can therefore be caused indirectly by M2 macrophages. These macrophages could give stimulatory factors to the human synovial fibroblasts that are cultured in the same compartment. These stimulatory factors of M2 macrophages stimulate tissue regeneration and thus collagen I production is upregulated. The same is seen for M2 macrophages in coculture with laryngotracheal stenosis fibroblasts [46]. HUVEC cells are most likely not directly the cause of a higher production of collagen I, as a non-permeable PDMS membrane is in between the two compartments and HUVEC cells are seeded in the compartment below the fibroblasts and macrophages. Cell to cell communication is therefore not possible between fibroblasts and HUVEC cells. However, molecules that have a NO comparable size can pass through the membrane and affect the fibroblast and macrophage layer. Thus, only molecules of the size of NO that could potentially have an effect on macrophage polarization should

be taken into account too.
As can be seen in figure 15, hyaluronan synthase 1 is clearly visible inside the cells. Hyaluronic acid is one of the important components of synovial fluid, discussed in section 1.1 [11] [47]. Hyaluronic Acid is produced partly by HAS1. This indicates that the human synovial fibroblasts seeded still do one of their primary tasks, while in the high NO concentration double culture on day 10. If human synovial fibroblasts still can produce hyaluronic acid in even higher NO concentrations or in samples with low NO levels could give insight in the effect of NO on synovial fibroblasts.
Moreover, a decrease in $CD163^{+}/DAPI^{+}$ ratio is seen for double culture samples, while triple culture samples show an increase in $CD163^{+}/DAPI^{+}$ ratio (figure 16). This means that there seems to be more M2 macrophages, if the ratio between macrophages and fibroblasts stays the same over the days.
In figure 17b and 17d, a confluent and packed layer of HUVECs can be seen. The same day as this layer becomes confluent, NO concentrations drop to a low level. According to those results, a confluent and packed layer HUVECs lowers the concentration of NO in the samples. As discussed, only small molecules can cause cross-talk between the HUVEC layer and the fibroblasts and macrophage layer and NO levels of HUVECs cannot influence the levels of NO in the top compartment of the compartment. This indicates that another small molecule passes through the PDMS layer and lowers NO levels in the top compartment. Another possibility could be that nitrite (NO_2) levels are lowered, by a reaction caused by HUVECs. Why NO levels are lower in samples with HUVECs should still be discussed and studied.
Unfortunately, CD68 and CD80 staining stained aspecific or did not give any signal. Why this happened, remained unclear during and after the project.

4.4 qPCR results

As can be seen in figure 19, 20 and 21, error bars are high and data points vary for qPCR results. This could indicate that some data points are not valid, or others are just not produced correctly. This could lead to unreliable results. For example, collagen I expression shown in figure 19 has very high values for double culture samples on day 6. These values are higher when compared to the other conditions. This sudden decrease in collagen I production from day 6 to day 10 does not seem reliable. This shows that some of the data is not correct or cannot be relied upon.
Moreover, results presented in figure 20 for *IL1R* expression show high expression in synovial fibroblasts seeded only samples. This is unexpected, as this primer is chosen to be only expressed in macrophages. However, as literature shows, *IL1R* is expressed in both normal and osteoarthritis human synovial fibroblasts. [48]. Furthermore, *CD80* showed unexpected results. For triple culture samples on day 6, a relatively low expression is found. However, a substantial increase is seen on day 10 for triple culture samples. This can be due to homeostasis of the balance of M1 macrophages to M2 macrophages. Homeostasis of both sides of macrophages is critical in the body [49]. Without a balance of M1/M2 macrophage types, irregular processes can take place. For example, only M1 macrophages in our body will cause an inflammation that keeps on getting more inflamed. Only M2 macrophages will cause abnormal tissue growth, as M2 macrophages will stimulate tissue regeneration. Tissue balance is therefore done by macrophages, as a balance between the two forms will keep the tissue in balance. An increase of *CD80* (so an increase in M1 macrophages) could therefore be expected on day 10, where a substantial increase is also seen in *CD163* and *TLR1* (M2 markers, figure 21) and high proliferative activity is seen. Also, *iNOS* expression showed a high increase on day 10. A high standard deviation is seen for this condition, which indicates high variety between measurements. While Griess assay results showed low NO concentrations for this condition, a large increase in *iNOS* is therefore unexpected. The membrane between samples could therefore be broken, which results in direct cross-talk and cell-to-cell contact of HUVECs and the synovial fibroblast and macrophage layer resulting in unexpected results in line with the report.
In figure 21, similar results are seen as for section 3.1. As said in section 4.1, poorly integrated macrophages indicate M1 macrophages. A good integrated layer of macrophages inside the human synovial fibroblasts layer can be seen as resting macrophages. Resting macrophages are more prone for not inflamed cultures, which means that M2 macrophage polarization would be more argumentative. *CD163* and *TLR1* expression graphs in figure 21 confirm this statement, as these markers for M2 macrophages are increasing in HUVEC+ samples on day 10. Moreover, an increase is seen for double culture samples. This could again be due by an attempt of homeostasis of the system. This increase for double culture samples on day 10, however, is significantly

lower than triple culture samples. This will create two conditions, whereas one of them has a significantly low concentration of NO on day 10 for triple culture samples and a significantly high concentration of NO on day 10 for double culture samples.

4.5 Other recommendations

Usage of MMPs could potentially give an insight into which signal cascades are influenced by NO. With this information, a conclusion could be further made for how NO influences the polarization of macrophages as NO could have an influence on MMP production. This can be done by

5 Conclusion

For this project, the effect of nitric oxide on macrophage polarization in the synovial membrane was studied. The wide range of experiments done shows results of a double compartment synovial membrane-on-chip system with culture up to 10 days.

Griess assay showed an increasing difference of NO concentration between both double and triple culture samples. On day 10, double culture samples had a higher concentration, while triple culture samples had a low concentration of NO compared to double culture samples. NO concentrations are stable between day 6 and day 8 in triple culture systems, followed by a significant decrease between day 8 and 10 of the experiment. Double culture samples showed an increase in NO concentration between day 6 and 8, while remaining constant levels between day 8 and 10.

Furthermore, it can be concluded that the amount of collagen I increased over the days for all conditions. Collagen I showed clusters for triple culture samples on day 10. Also, HAS1 is a potential marker for synovial fibroblasts as it produces hyaluronic acid, a key component of synovial fibroblast. More M2 macrophages are seen in triple culture samples, than double culture samples. while a decrease is seen in double culture samples. HUVEC cells showed a higher confluency and a dense structure on day 10, with respect to day 6.

For high levels of NO, *COL1A1* and *SPHK1* were decreased. *COL6A1*, *IL1R*, *CD80*, *iNOS* and *TLR1* increased. Next, *HAS1* and *CD163* remained stable.

For low levels of NO, *COL1A1*, *HAS1* and *IL1R* decreased. *CD80*, *iNOS* and all M2 markers studied (*CD163*, *SPHK1* and *TLR1*) increased. Furthermore, *COL6A1* remained stable.

Overall, a high NO concentration is coupled with a polarization to M1 macrophages and a low NO concentration is coupled with a polarization to M2 macrophages. Still many variables have to be discussed before claiming a causal relationship between NO and macrophage polarization.

6 Acknowledgements

Without the support of many people around me, this report could not be possible to produce. Support in thought processes, assistance with lab work or providing me with the materials for this interesting project has all been needed to produce the results that is described and elaborated on in this report. In this section, I would like to thank the numerous people that helped me throughout this project, which may not all be individually mentioned in this section.

First and foremost, I would like to thank my daily supervisor Carlo Alberto Paggi. Already on the very start of this project, he encouraged me to work on it. Whenever I lost motivation during the project, he knew exactly how to motivate me again. As a starter in the world of science, it can sometimes be hard to stay motivated after unfavourable results. He could then get me inspired again to produce even better results. Moreover, I started this project as a person that disliked presenting for a big group. He has persuaded me to like presenting and even changed me into a person that can present with passion. Furthermore, as science sometimes can get boring, he made me laugh at the right times. This kept me motivated through the project and work hard to produce these astonishing results. Your positivity, cheerfulness and very supporting character will not soon be forgotten.

Second, I would like to thank Marcel Karperien for giving me the opportunity to work on this fascinating project. In the orientation phase of the project, he inspired me to start on this fascinating project. Also, he trusted me to finish this project with the best results. Your trust and help are much appreciated.

Third, I would like to thank Nuno Araújo Gomes & Agnieszka Zuchowska for providing me with the cells needed to do this project. Nuno Araújo Gomes provided me with THP-1 monocytes and helped me with working with monocytes and macrophages. Moreover, he still trusted me with his monocytes even after over-confluenting a cell culture of monocytes. Your trust in me and the maty conversations at the labs are so much appreciated
Agnieszka Zuchowska provided me with HUVEC cells and helped me to culture and seed them properly in a microfluidic chip system. Also, she always was there to help me out whenever Carlo was not available at that time. Also, the fun times and delicious Polish cake at the coffee break will soon not be forgotten.

Next, I would like to thank Daniel Brommer. He did a similar project, as we both used the system designed by C.A. Paggi. This meant that we had to go through the same struggles, which have created some very funny but also educational moments. He was there when I could not do my tasks because of any private circumstances. Moreover, numerous interesting, hilarious and helpful conversations were held during this project with Daniel. These conversations are too many to remember, but I still would like to take this moment to show my appreciation for all of the moments that took place between us. He took this already very fun and educational period to another level.

Last, but certainly not least, I would like to thank all DBE members and others that helped me throughout the whole project. Without your help, these results would never be possible to have. I would like to express my gratitude specifically to Simon, Thomas and Renata. These three Master Students worked the closest with my project and were always there if I needed help. Also, when needed they could supply me with the necessary products and elements for this project. The always open and friendly characters of you all has felt special to me.

A Appendix

A.1 Immunofluorescence pictures

A.1.1 Collagen 1

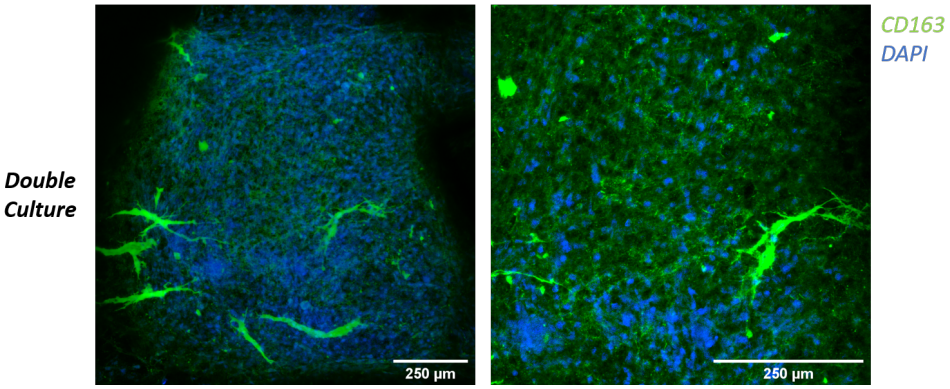

Figure 22: Top view of the synovial fibroblast and macrophage layer with collagen I (in green) and DAPI (in blue) of double culture samples on day 10. Scale bar: 250 µm

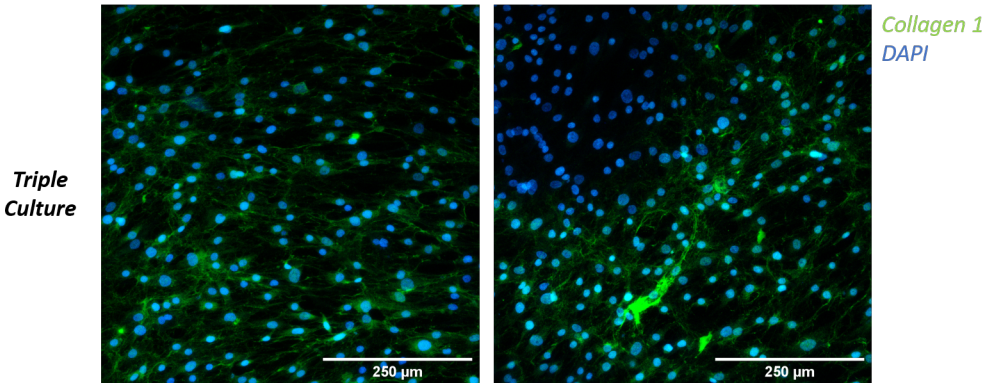

Figure 23: Top view of the synovial fibroblast and macrophage layer with collagen I (in green) and DAPI (in blue) of triple culture samples on day 6. Scale bar: 250 µm

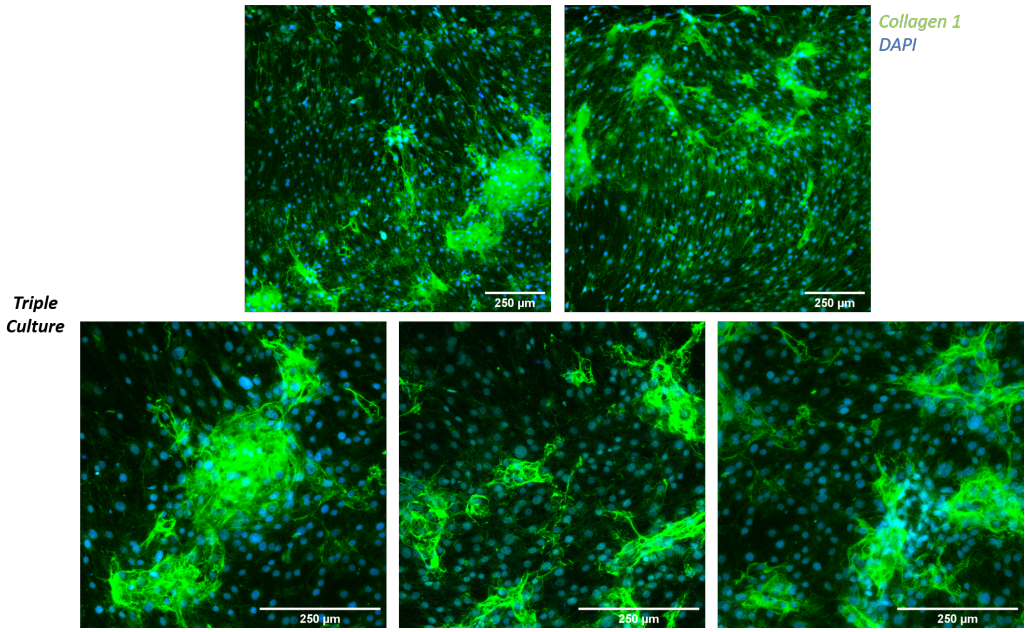

Figure 24: Top view of the synovial fibroblast and macrophage layer with collagen I (in green) and DAPI (in blue) of triple culture samples on day 10. Scale bar: 250 µm

A.1.2 Col6A1

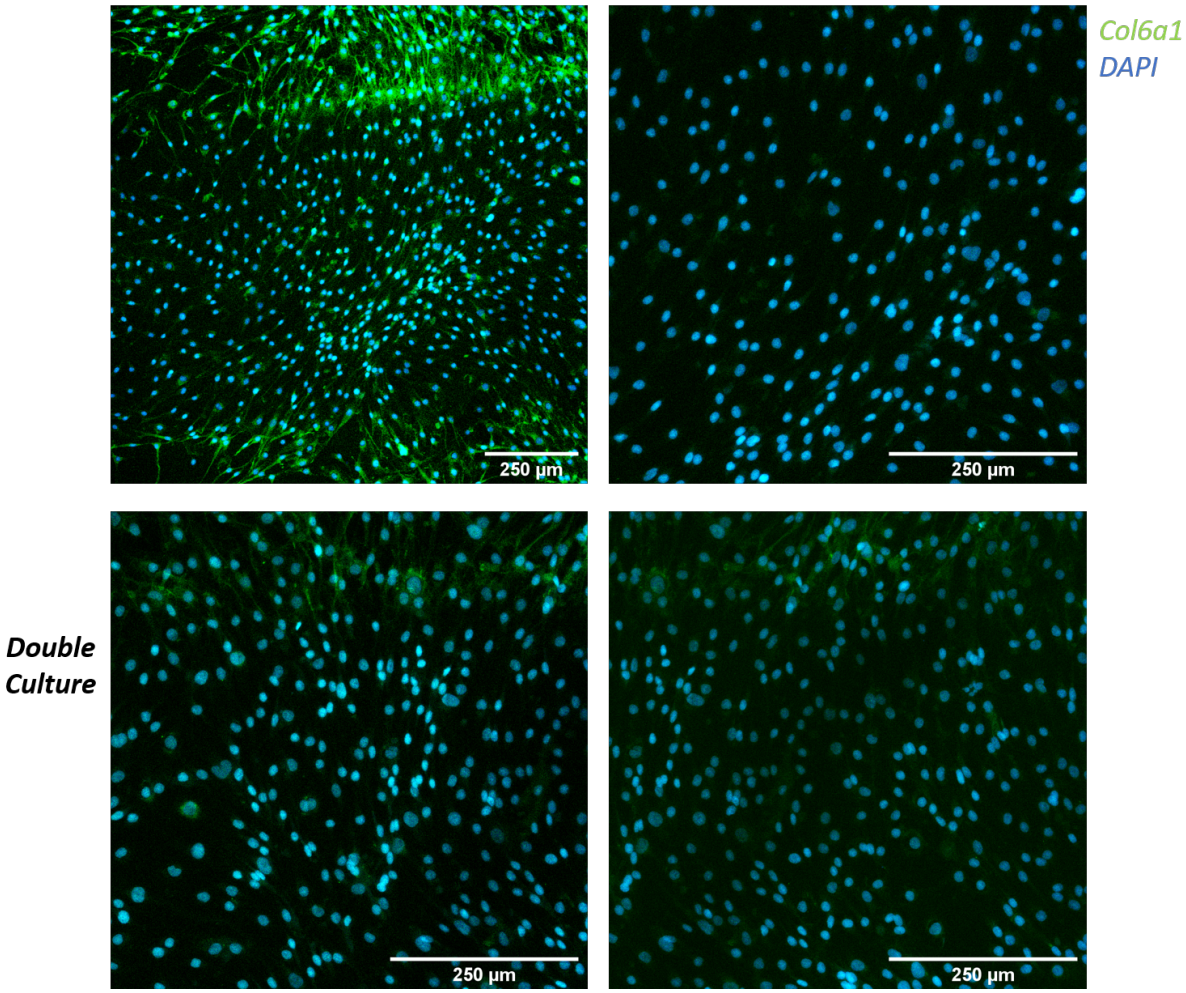

Figure 25: Top view of the synovial fibroblast and macrophage layer with collagen 6 (in green) and DAPI (in blue) of double culture samples on day 10. Scale bar: 250 µm

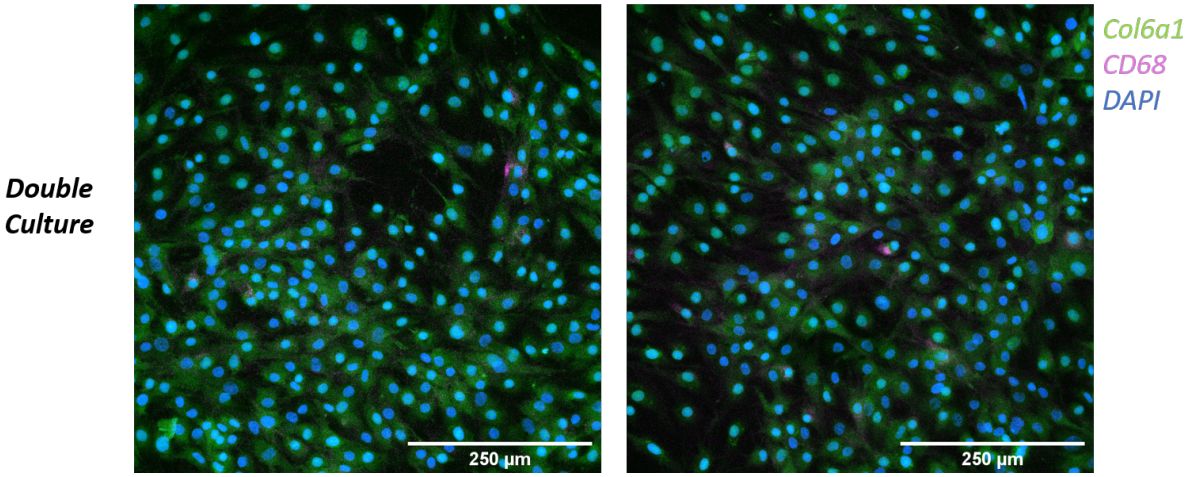

Figure 26: Top view of the synovial fibroblast and macrophage layer with CD68 (in magenta), collagen 6 (in green) and DAPI (in blue) of double culture samples on day 10. Scale bar: 250 µm

A.1.3 CD163

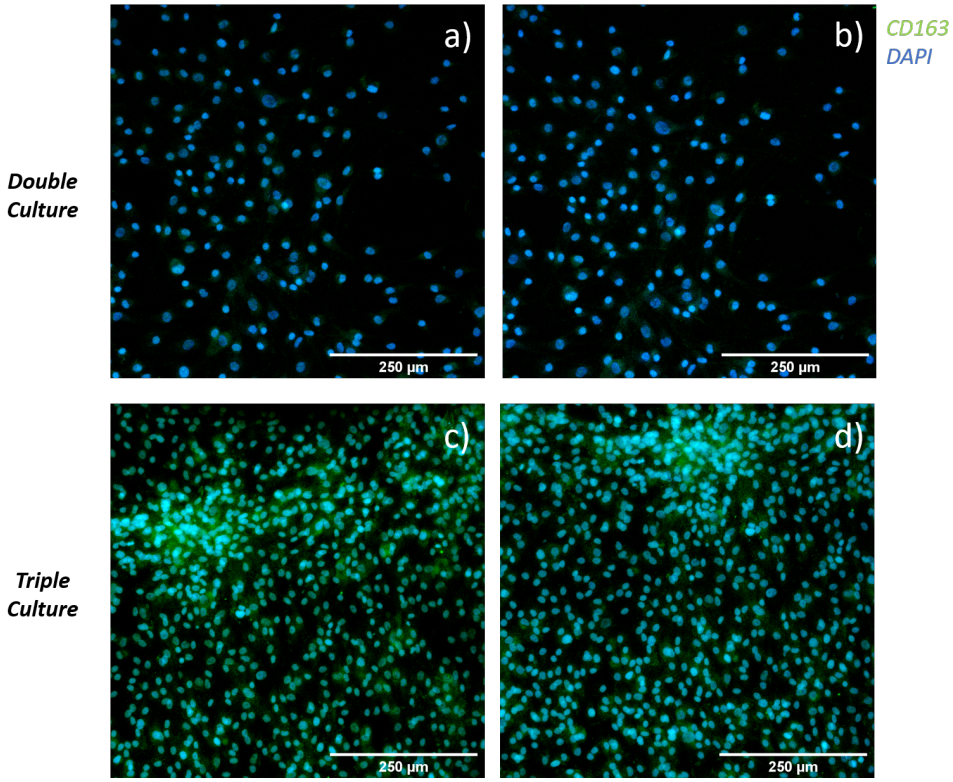

Figure 27: Top view of the synovial fibroblast and macrophage layer with CD163 (in green) and DAPI (in blue) of double culture samples (top) and triple culture samples (bottom) on day 6. Scale bar: 250 µm

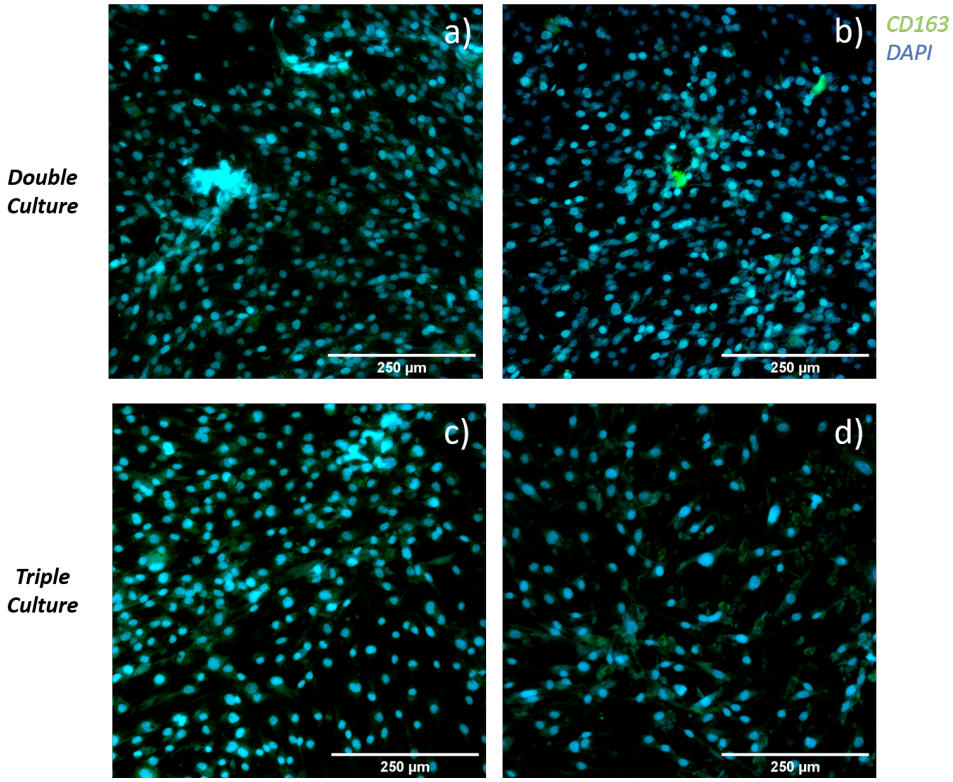

Figure 28: Top view of the synovial fibroblast and macrophage layer with CD163 (in green) and DAPI (in blue) of double culture samples (top) and triple culture samples (bottom) on day 10. Scale bar: 250 µm

A.1.4 Phalloidin

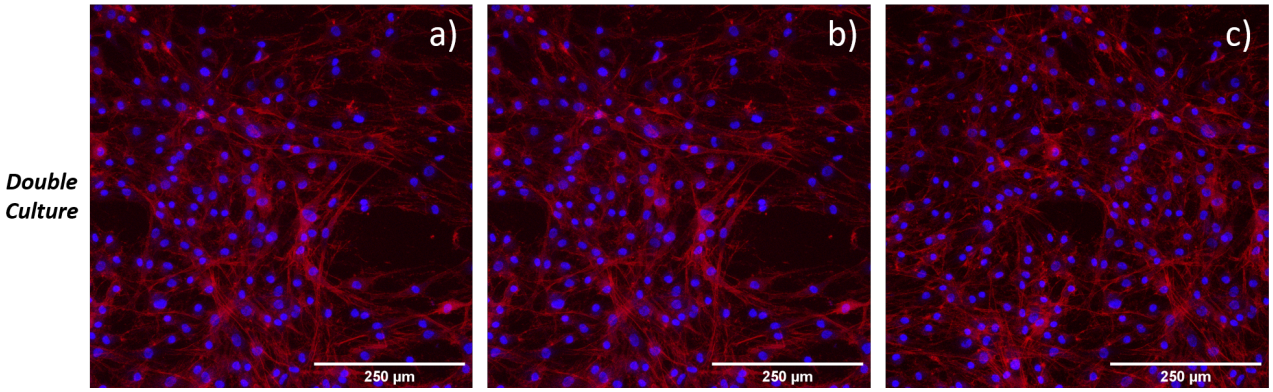

Figure 29: Top view of the synovial fibroblast and macrophage layer with Phalloidin (in red) and DAPI (in blue) of double culture samples on day 6. Scale bar: 250 µm

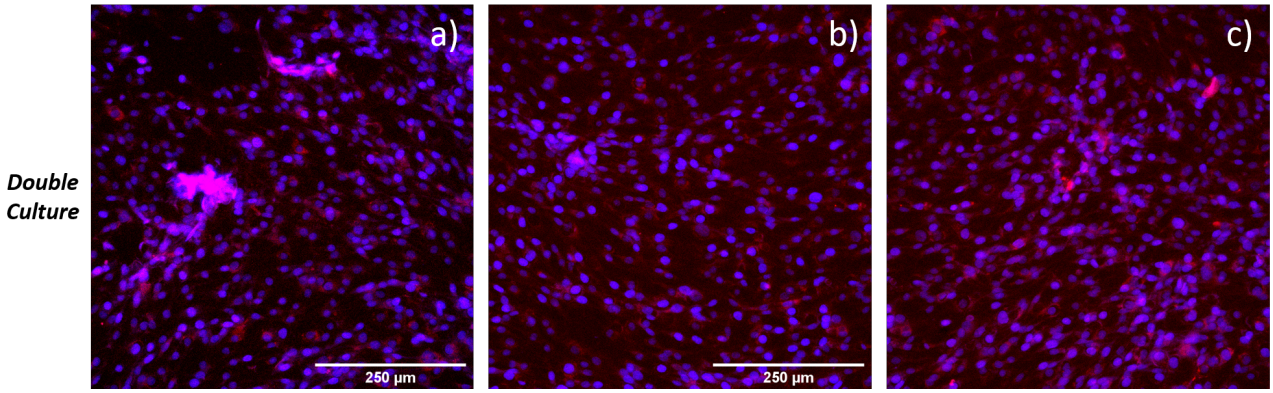

Figure 30: Top view of the synovial fibroblast and macrophage layer with Phalloidin (in red) and DAPI (in blue) of double culture samples on day 10. Scale bar: 250 µm

A.1.5 HUVECs

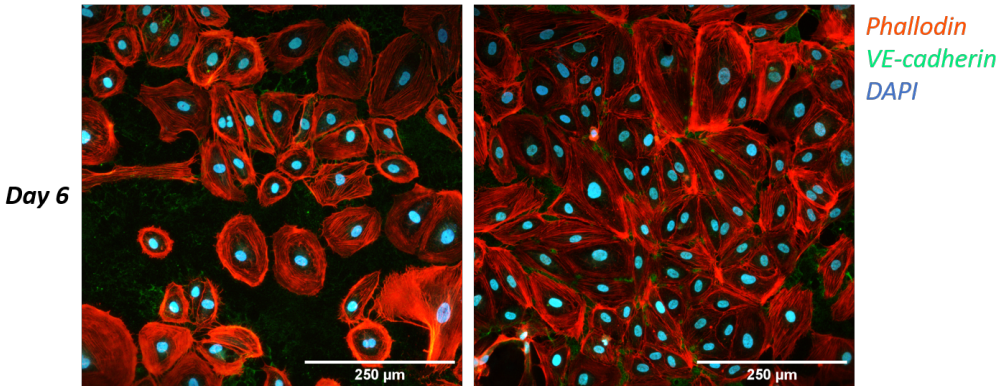

Figure 31: Top view of the HUVEC layer with Phalloidin (in red), VE-cadherin (in green) and DAPI (in blue) of triple culture samples on day 6. Scale bar: 250 µm

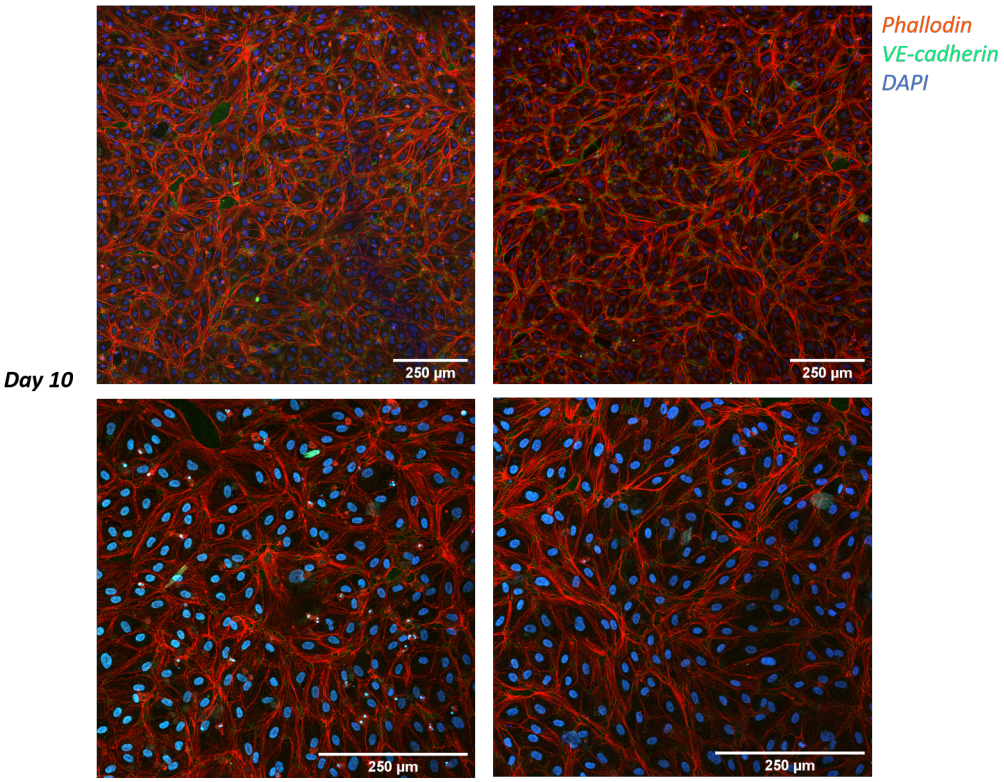

Figure 32: Top view of the HUVEC layer with Phalloidin (in red), VE-cadherin (in green) and DAPI (in blue) of triple culture samples on day 10. Scale bar: 250 µm

A.2 qPCR primer sequences

Primer	Forward sequence	Reverse sequence	Target
GAPDH	CGCTCTCTGCTCCTCCTGTT	CCATGGTGTCTGAGCGATGT	Reference gene
COL1A1	GTCACCCACCGACCAAGAAACC	AAGTCCAGGCTGTCCAGGGATG	ECM
COL6A1	CTGGGCGTCAAAGTCTTCTC	ATTCGAAGGAGCAGCACACT	ECM
HAS1	CGCTAACTACGTCCCTCTGC	CCAGTACAGCGTCAACATGG	ECM
CD80	GGGAAAGTGTACGCCCTGTA	GCTACTTCTGTGCCCACCAT	M1
IL1R	TATGCCTCATGCTGACTTGC	CTCTGGTGATCCACCCACTT	M1
iNOS	GCTCTACACCTCCAATGTGACC	CTGCCGAGATTTGAGCCTCATG	M1
CD163	TTGCCAGCAGCTTAAATGTG	AGGACAGTGTTTGGGACTGG	M2a and M2c
CD200R	GTTGCCCTCCTATCGCATTA	TGGAAATTCCCATCAGGTGT	M2a
SPHK1	ACCCATGAACCTGCTGTCTC	CAGGTGTCTTGGAACCCACT	M2b
TLR1	GGGTCAGCTGGACTTCAGAG	AAAATCCAAATGCAGGAACG	M2c
TLR8	TCCTTCAGTCGTCAATGCTG	CGTTTGGGGAACTTCCTGTA	M2c
IL10	TGGTGAAACCCCGTCTCTAC	CTGGAGTACAGGGGCATGAT	M2

Table 3: Table of qPCR primer sequences with their targets

References

[1] David J. Hunter, Lyn March, and Mabel Chew. Osteoarthritis in 2020 and beyond: a Lancet Commission. *The Lancet*, 396(10264):1711–1712, 2020. ISSN 1474547X. doi: 10.1016/S0140-6736(20)32230-3. URL http://dx.doi.org/10.1016/S0140-6736(20)32230-3.

[2] Khalid Almutairi, Johannes Nossent, David Preen, Helen Keen, and Charles Inderjeeth. The global prevalence of rheumatoid arthritis: a meta-analysis based on a systematic review. *Rheumatology International*, 41(5):863–877, 2021. ISSN 1437160X. doi: 10.1007/s00296-020-04731-0. URL https://doi.org/10.1007/s00296-020-04731-0.

[3] Petra. Eysink, René. Poos, Gool Coen Van, Hilderink Henk Kommer Geert Jan, Mulder Maarten, and Gijsen Ronald. Epidemiologische data van ziekten van het botspierstelsel en bindweefsel. *Achtergrondrapport Zorg*, page 102, 2019.

[4] Reumatoïde artritis (RA) | Cijfers & Context | Huidige situatie | Volksgezondheidenzorg.info, . URL https://www.volksgezondheidenzorg.info/onderwerp/reumato{ï}de-artritis-ra/cijfers-context/huidige-situatie#!node-prevalentie-reumato{ï}de-artritis-huisartsenpraktijk.

[5] Artrose | Cijfers & Context | Huidige situatie | Volksgezondheidenzorg.info, . URL https://www.volksgezondheidenzorg.info/onderwerp/artrose/cijfers-context/huidige-situatie#node-prevalentie-en-aantal-nieuwe-gevallen-van-artrose-huisartsenpraktijk.

[6] Elaine Thomas, George Peat, and Peter Croft. Defining and mapping the person with osteoarthritis for population studies and public health. *Rheumatology (United Kingdom)*, 53(2):338–345, 2014. ISSN 14620324. doi: 10.1093/rheumatology/ket346.

[7] Carl Orr, Elsa Sousa, David L. Boyle, Maya H. Buch, Christopher D. Buckley, Juan D. Cañete, Anca I. Catrina, Ernest H.S. Choy, Paul Emery, Ursula Fearon, Andrew Filer, Danielle Gerlag, Frances Humby, John D. Isaacs, Søren A. Just, Bernard R. Lauwerys, Benoit Le Goff, Antonio Manzo, Trudy McGarry, Iain B. McInnes, Aurélie Najm, Constantino Pitzalis, Arthur Pratt, Malcolm Smith, Paul P. Tak, Rogier Thurlings, João E. Fonseca, and Douglas J. Veale. Synovial tissue research: A state-of-the-art review. *Nature Reviews Rheumatology*, 13(8):463–475, 2017. ISSN 17594804. doi: 10.1038/nrrheum.2017.115.

[8] Cristina Manferdini, Yasmin Saleh, Paolo Dolzani, Elena Gabusi, Diego Trucco, Giuseppe Filardo, and Gina Lisignoli. a Preclinical Synovial Fibroblasts / Macrophages in an In Vitro Model of Osteoarthritis. pages 1–20, 2020.

[9] Graeme Jones, Peter Nash, and Stephen Hall. Advances in rheumatoid arthritis. *Medical Journal of Australia*, 206(5):221–224, 2017. ISSN 13265377. doi: 10.5694/mja16.01287.

[10] Pavlos Bobos, Joy C. Macdermid, Goris Nazari, Emily A. Lalone, Louis Ferreira, and Ruby Grewal. Joint protection programmes for people with osteoarthritis and rheumatoid arthritis of the hand: An overview of systematic reviews. *Physiotherapy Canada*, 73(1):56–65, 2021. ISSN 03000508. doi: 10.3138/ptc-2019-0037.

[11] Elaine Nicpon Marieb and Katja Hoehn. *Human Anatomy & Physiology*, volume 10th Editi. Pearson Education Limited, 2016.

[12] Anthony L Mescher. *Junqueira's Basic Histology, Text & Atlas*, volume 1. McGraw-Hill Education, 13th edition, 2013. ISBN 9780071807203. doi: 10.1517/14728222.1.1.267.

[13] Malcolm D Smith. Suppl 1: the normal synovium. *The open rheumatology journal*, 5:100, 2011.

[14] Arjen B. Blom and Wim B. van den Berg. The Synovium and Its Role in Osteoarthritis. *Bone and Osteoarthritis*, pages 65–79, 2007. doi: 10.1007/978-1-84628-701-5_4.

[15] Roxana Monemdjou, Hassan Fahmi, and Mohit Kapoor. Synovium in the pathophysiology of osteoarthritis. *Therapy*, 7(6):661–668, 2010. ISSN 14750708. doi: 10.2217/thy.10.72.

[16] M. J. Benito, D. J. Veale, O. FitzGerald, W. B. Van Den Berg, and B. Bresnihan. Synovial tissue inflammation in early and late osteoarthritis. *Annals of the Rheumatic Diseases*, 64(9):1263–1267, 2005. ISSN 00034967. doi: 10.1136/ard.2004.025270.

[17] Piotr Wojdasiewicz, Łukasz A. Poniatowski, and Dariusz Szukiewicz. The role of inflammatory and anti-inflammatory cytokines in the pathogenesis of osteoarthritis. *Mediators of Inflammation*, 2014, 2014. ISSN 14661861. doi: 10.1155/2014/561459.

[18] Fionula M. Brennan and Iain B. McInnes. Evidence that cytokines play a role in rheumatoid arthritis. *Journal of Clinical Investigation*, 118(11):3537–3545, 2008. ISSN 00219738. doi: 10.1172/JCI36389.

[19] J. Furuzawa-Carballeda and Jorge Alcocer-Varela. Interleukin-8, interleukin- 10, intercellular adhesion molecule- 1 and vascular cell adhesion molecule-1 expression levels are higher in synovial tissue from patients with rheumatoid arthritis than in osteoarthritis. *Scandinavian Journal of Immunology*, 50(2): 215–222, 1999. ISSN 03009475. doi: 10.1046/j.1365-3083.1999.00573.x.

[20] Marc Feldmann, Fionula M. Brennan, and Ravinder N. Maini. Role of cytokines in rheumatoid arthritis. *Annual Review of Immunology*, 14:397–440, 1996. ISSN 07320582. doi: 10.1146/annurev.immunol.14.1.397.

[21] M.F. Pustjens, S.C. Mastbergen, N. Eijkelkamp, and F.P. Lafeber. Expression of GM-CSF and its receptor CD116 in the synovium of OA patients is negatively correlated with pain. *Osteoarthritis and Cartilage*, 24(2016):S454–S455, 2016. ISSN 10634584. doi: 10.1016/j.joca.2016.01.829. URL http://dx.doi.org/10.1016/j.joca.2016.01.829.

[22] Yongli Yao, Xiang-hong Xu, and Liping Jin. Macrophage Polarization in Physiological and Pathological Pregnancy. 10(April):1–13, 2019. doi: 10.3389/fimmu.2019.00792.

[23] Chen Yunna, Hu Mengru, Wang Lei, and Chen Weidong. Macrophage M1 / M2 polarization. *European Journal of Pharmacology*, 877(March):173090, 2020. ISSN 0014-2999. doi: 10.1016/j.ejphar.2020.173090. URL https://doi.org/10.1016/j.ejphar.2020.173090.

[24] Peter J Murray. Macrophage Polarization. (October), 2016. doi: 10.1146/annurev-physiol-022516-034339.

[25] Anastasiya S. Poltavets, Polina A. Vishnyakova, Andrey V. Elchaninov, Gennady T. Sukhikh, and Timur Kh. Fatkhudinov. Macrophage Modification Strategies for Efficient Cell Therapy. pages 1–19, 2020.

[26] Marie Genin, Francois Clement, Antoine Fattaccioli, Martine Raes, and Carine Michiels. M1 and M2 macrophages derived from THP-1 cells differentially modulate the response of cancer cells to etoposide. pages 1–14, 2015. doi: 10.1186/s12885-015-1546-9.

[27] Alexandra Damerau and Timo Gaber. Modeling Rheumatoid Arthritis In Vitro : From Experimental Feasibility to Physiological Proximity. 2020.

[28] Bruce Alberts, Dennis Bray, Karen Hopkin, Alexander Johnson, Julian Lewis, Martin Raff, Keith Roberts, and Peter Walter. *Essential Cell Biology*. Garland Science, New York, 4th edition, 2014. ISBN 9780815344544.

[29] Paula Yurkanis Bruice. *Organic Chemistry*. Pearson Education Limited, Santa Barbara, 2017. ISBN 9780134042282.

[30] Nancy L Mccartney-francis, Xiao-yu Song, Diane E Mizel, and Sharon M Wahl. Selective Inhibition of Inducible Nitric Oxide Synthase Exacerbates Erosive Joint Disease. 2021. doi: 10.4049/jimmunol.166.4.2734.

[31] Richard Graham Knowles. The role of nitric oxide in osteoarthritis. (April 2018), 2007. doi: 10.1080/03009740701483014.

[32] Sue-jie Koo and Nisha J Garg. Redox Biology Metabolic programming of macrophage functions and pathogens control. *Redox Biology*, 24(April):101198, 2019. ISSN 2213-2317. doi: 10.1016/j.redox.2019.101198. URL https://doi.org/10.1016/j.redox.2019.101198.

[33] Gaoxing Luo, Daizhi Peng, Junsong Zheng, Xiwei Chen, and Jun Wu. The role of NO in macrophage dysfunction at early stage after burn injury. 31:138–144, 2005. doi: 10.1016/j.burns.2004.09.009.

[34] A Perner, L Andresen, M Normark, and S Sørensen. Expression of nitric oxide synthases and e V ects of L -arginine and L -NMMA on nitric oxide production and fluid transport in collagenous colitis. (x): 387–394, 2001.

[35] R J Van Hof, L Hocking, P K Wright, and S H Ralston. Nitric oxide is a mediator of apoptosis in the rheumatoid joint. pages 1004–1008, 2000.

[36] Iain B. McInnes, Bernard P. Leung, Max Field, and Xiao Q. Wei. Production of Nitric Oxide in the Synovial Membrane of Rheumatoid and Osteoarthritis Patients. 1996.

[37] Weilue He and Megan C Frost. Redox Biology CellNO trap : Novel device for quantitative , real-time , direct measurement of nitric oxide from cultured RAW 267 . 4 macrophages. *Redox Biology*, 8:383–397, 2016. ISSN 2213-2317. doi: 10.1016/j.redox.2016.03.006. URL http://dx.doi.org/10.1016/j.redox.2016.03.006.

[38] Diane E Handy Rita Castro Joseph Loscalzo. Methods to Detect Nitric Oxide and its Metabolites in Biological Samples. *Bone*, 23(1):1–7, 2011. ISSN 6176321972.

[39] Hasmik Jasmine Samvelyan, David Hughes, Craig Stevens, and Katherine Ann Staines. Models of Osteoarthritis: Relevance and New Insights. *Calcified Tissue International*, (0123456789), 2020. ISSN 14320827. doi: 10.1007/s00223-020-00670-x. URL https://doi.org/10.1007/s00223-020-00670-x.

[40] Mario Rothbauer, Gregor Höll, Christoph Eilenberger, Sebastian R.A. Kratz, Bilal Farooq, Patrick Schuller, Isabel Olmos Calvo, Ruth A. Byrne, Brigitte Meyer, Birgit Niederreiter, Seta Küpcü, Florian Sevelda, Johannes Holinka, Oliver Hayden, Sandro F. Tedde, Hans P. Kiener, and Peter Ertl. Monitoring tissue-level remodelling during inflammatory arthritis using a three-dimensional synovium-on-a-chip with non-invasive light scattering biosensing. *Lab on a Chip*, 20(8):1461–1471, 2020. ISSN 14730189. doi: 10.1039/c9lc01097a.

[41] John C Krebs, Yunus Alapan, Barbara A Dennstedt, Glenn D Wera, and Umut A Gurkan. Microfluidic processing of synovial fluid for cytological analysis. 2017. doi: 10.1007/s10544-017-0163-6.

[42] Promega Corporation, K M Miranda, M G Espey, and D a Wink. Griess Reagent System. *Nitric oxide : biology and chemistry / official journal of the Nitric Oxide Society*, 5(1):7, 2009. ISSN 1089-8603. doi: 10.1006/niox.2000.0319.

[43] Fiona J Pixley. Macrophage Migration and Its Regulation by CSF-1. *International Journal of Cell Biology*, 2012:501962, 2012. ISSN 1687-8876. doi: 10.1155/2012/501962. URL https://doi.org/10.1155/2012/501962.

[44] Kui Cui, Christopher L. Ardell, Nataly P. Podolnikova, and Valentin P. Yakubenko. Distinct migratory properties of M1, M2, and resident macrophages are regulated by αdβ2and αmβ2integrin-mediated adhesion. *Frontiers in Immunology*, 9(NOV):1–14, 2018. ISSN 16643224. doi: 10.3389/fimmu.2018.02650.

[45] Kyle William Evans. PPAR gamma and eNOS contribute to the resolution of chronic inflammation. *Temple University Graduate Board*, 2012.

[46] Kevin Motz, Ioan Lina, Michael K. Murphy, Virginia Drake, Ruth Davis, Hsiu Wen Tsai, Michael Feeley, Linda X. Yin, Dacheng Ding, and Alexander Hillel. M2 Macrophages Promote Collagen Expression and Synthesis in Laryngotracheal Stenosis Fibroblasts. *Laryngoscope*, 131(2):E346–E353, 2021. ISSN 15314995. doi: 10.1002/lary.28980.

[47] Nguyet Nguyen, Awanit Kumar, Simi Chacko, Rodney J. Ouellette, and Anirban Ghosh. Human hyaluronic acid synthase-1 promotes malignant transformation via epithelial-to-mesenchymal transition, micronucleation and centrosome abnormalities. *Cell Communication and Signaling*, 15(1):1–13, 2017. ISSN 1478811X. doi: 10.1186/s12964-017-0204-z.

[48] M'Bark Sadouk, Jean-Pierre Pelletier, Ginette Tardif, Kayghobad Kiansa, Jean-Marie Cloutier, and Johanne Martel-Pelletier. Human synovial fibroblasts coexpress il-1 receptor type i and type ii mrna. the increased level of the il-1 receptor in osteoarthritic cells is related to an increased level of the type i receptor. *Laboratory investigation; a journal of technical methods and pathology*, 73(3):347–355, 1995.

[49] Thomas a. Wynn, Ajay Chawla, and Jeffrey W. Pollard. Origins and Hallmarks of Macrophages: Development, Homeostasis, and Disease. *Nature*, 496(7446):445–455, 2013. ISSN 0028-0836. doi: 10.1038/nature12034.Origins.